Redox Biology 76 (2024) 103316

Contents lists available at ScienceDirect

Redox Biology

journal homepage: www.elsevier.com/locate/redox

Heme: A link between hemorrhage and retinopathy of prematurity progression

Tamás Gáll [a,1], Dávid Pethő [a,b,c,1], Katalin Erdélyi [d], Virág Egri [e], Józon György Balla [f], Annamária Nagy [a,b], Annamária Nagy [g], Szilárd Póliska [h], Magnus Gram [i,j,p], Róbert Gábriel [k,l], Péter Nagy [d,m,o], József Balla [a,b], György Balla [a,n,*]

[a] Department of Internal Medicine, Division of Nephrology, Faculty of Medicine, University of Debrecen, Debrecen, H-4032, Hungary
[b] HUN-REN–UD Vascular Biology and Myocardium Pathophysiology Research Group, Hungarian Academy of Sciences, University of Debrecen, Debrecen, H-4032, Hungary
[c] Kálmán Laki Doctoral School, University of Debrecen, Debrecen, Hungary
[d] Department of Molecular Immunology and Toxicology and the National Tumor Biology Laboratory, National Institute of Oncology, Budapest H-1122, Hungary
[e] Faculty of Medicine, University of Debrecen, Debrecen, H-4032, Hungary
[f] Department of Laboratory Medicine, Faculty of Medicine, University of Debrecen, Debrecen, H-4032, Hungary
[g] Department of Ophthalmology, Faculty of Medicine, University of Debrecen, Debrecen H-4032, Hungary
[h] Genomic Medicine and Bioinformatic Core Facility, Department of Biochemistry and Molecular Biology, Faculty of Medicine, University of Debrecen, Debrecen, H-4032, Hungary
[i] Pediatrics, Department of Clinical Sciences Lund, Lund University, Lund, Sweden
[j] Department of Neonatology, Skåne University Hospital, Lund, Sweden
[k] Department of Experimental Zoology and Neurobiology, University of Pécs, Pécs, H-7624, Hungary
[l] János Szentágothai Research Centre, University of Pécs, Pécs, H-7624, Hungary
[m] Chemistry Institute, University of Debrecen, Debrecen, H-4032, Hungary
[n] Department of Pediatrics, Faculty of Medicine, University of Debrecen, Debrecen, H-4032, Hungary
[o] Department of Anatomy and Histology, HUN-REN-UVMB Laboratory of Redox Biology, University of Veterinary Medicine; Budapest, Hungary
[p] Biofilms – Research Center for Biointerfaces, Department of Biomedical Science, Faculty of Health and Society, Malmö University, Malmö, Sweden

ARTICLE INFO

Keywords:
Retinopathy
Heme
VEGF
Hypoxia
Rapamycin
Mitochondria

ABSTRACT

Neovascularization is implicated in the pathology of retinopathy of prematurity (ROP), diabetic retinopathy (DR), and age-related macular degeneration (AMD), which are the leading causes of blindness worldwide. In our work, we analyzed how heme released during hemorrhage affects hypoxic response and neovascularization. Our retrospective clinical analysis demonstrated, that hemorrhage was associated with more severe retinal neovascularization in ROP patients. Our heme-stimulated human retinal pigment epithelial (ARPE-19) cell studies demonstrated increased expression of positive regulators of angiogenesis, including vascular endothelial growth factor-A (VEGFA), a key player of ROP, DR and AMD, and highlighted the activation of the PI3K/AKT/mTOR/VEGFA pathway involved in angiogenesis in response to heme. Furthermore, heme decreased oxidative phosphorylation in the mitochondria, augmented glycolysis, facilitated HIF-1α nuclear translocation, and increased VEGFA/GLUT1/PDK1 expression suggesting HIF-1α-driven hypoxic response in ARPE-19 cells without effecting the metabolism of reactive oxygen species. Inhibitors of HIF-1α, PI3K and suppression of mTOR pathway by clinically promising drug, rapamycin, mitigated heme-provoked cellular response. Our data proved that oxidatively modified forms of hemoglobin can be sources of heme to induce VEGFA during retinal hemorrhage. We propose that hemorrhage is involved in the pathology of ROP, DR, and AMD.

* Corresponding author. Department of Pediatrics, Faculty of Medicine, University of Debrecen, Debrecen, H-4032, Hungary.
E-mail address: balla@med.unideb.hu (G. Balla).
[1] These share the first authorship.

https://doi.org/10.1016/j.redox.2024.103316
Received 2 August 2024; Accepted 15 August 2024
Available online 16 August 2024

1. Introduction

Retina is one of the best vascularized human organ with two independent vascular systems [1]. The first system, known as the retinal circulation, is situated between the retinal nerve fiber layer and corpus vitreum. The second system, known as the choroidal circulation, is located beneath the retinal pigment epithelial cell layer. Vascular pathologies can lead to several age dependent retinal disorders. In the case of newborns, retinopathy of prematurity (ROP) has public health importance, while macular degeneration and diabetic retinopathy (DR) has significant danger for visual acuity of the middle age and older population [2]. The vascular pathology of these eye diseases often includes the growth of new blood vessels after the death and damage of existing vessels, furthermore, in ROP, the developmental perturbation is an extraordinary feature [3]. Retinal hemorrhage is often associated with these neovascularization [4]. The relationship between neovascularization and bleeding has remained unclear, and further investigation is needed to determine their potential role in the pathogenesis. To answer this dilemma, we selected two models for our study, a well characterized disease, ROP, to determine the importance of hemorrhage in neovascularization, and an in vitro retinal pigment epithelial cell culture system for studying the relationship between the regulation of angiogenesis and cellular heme stress.

ROP was first described and connected to premature birth in 1942 [5]. ROP, a retinal vasoproliferative eye disease affecting premature newborns, represents the most common cause of childhood blindness [6]. According to data from the Intelligent Research in Sight (IRIS) Registry in the United States, ROP causes 31.3 % of vision loss in children under the age of 18 years despite better understanding of the pathophysiology [7]. In Australia, ROP is the second most common diagnosis of ocular diseases in the first 3 years of life in a pediatric tertiary hospital [8].

The two phases of ROP pathophysiology are based on the retinal vascular development of premature newborns [9]. Expression of the two main ROP growth factors, vascular endothelial growth factor A (VEGFA) and insulin-like growth factor-1 (IGF-1), changes in parallel with the progression of these phases [10,11].

VEGFA is essential in retinal vascular development, since increasing oxygen demand of the neural retina generates VEGFA production in the retinal tissue [12]. Formation of new retinal vessels decreases hypoxia and VEGFA production after physiologic retinal vascularization [13]. In premature newborns, right after births, when the first phase of ROP starts, the extra uterine oxygen supply is pathologically high compared to the intrauterine milieu especially when therapeutic oxygen supplementation is justified. The relatively high oxygen supply interferes with the retinal vascular development by decreasing VEGFA expression and triggering partial vascular apoptosis of retinal vasculature [14]. The second phase of ROP is driven by tissue hypoxia; it is a consequence of vessel apoptosis and characterized by increased local VEGFA expression, resulting in pathological neovascularization a few weeks after birth [14]. In addition, other cell death mechanism, such as necroptosis and ferroptosis are also involved in ROP. Microglial necroptosis is involved in retinopathies and targeting microglial necroptosis can be a potential anti-angiogenesis therapy for retinal neovascular diseases [15]. Others have found that ferroptosis is involved in ROP, and ferroptosis inhibitor can alleviate retinal pathological angiogenesis in murine model of ROP [16].

Besides the importance of prematurity and oxygen, the first original publication also described the presence of retinal hemorrhage [5]. An association between hemorrhage and ROP severity has been raised earlier [4], but how hemorrhage can affect neovascularization has still remained ill-lit. In addition to ROP, DR is characterized by neovascularization, vascular fragility, and hemorrhages [17,18]. Extravasated red blood cells are susceptible to hemolysis; once oxidized, free hemoglobin releases its heme moieties, which have complex effects on surrounding cells and tissues [19–22].

In terms of ROP prevention, tightly controlled oxygen administration is a cornerstone of neonatal intensive care [23], but ROP remains a significant chronic disease. In addition to all this, the fact that ROP remains a significant issue for premature newborns is also supported by the following observation. In a prophylactic study, IGF-1 replacement immediately after birth did not significantly improve ROP, but prevented bronchopulmonary dysplasia, another chronic morbidity of premature infants, with 53–89 % efficacy [24]. Reducing pathologic neovascularization in the second phase is the main therapeutic approach of ROP today, which is based on neutralizing the proangiogenic effect of VEGFA in the retina [25]. Laser photocoagulation indirectly reduces VEGFA levels by ablating the peripheral avascular retina that produces the VEGFA [26], whereas intravitreal administration of VEGFA-specific antibodies bind retinal VEGFA [27].

Here, we combine clinical research with a physiologically relevant cell culture system to test the role of hemorrhage in the pathology of ROP. Together, the results provide mechanistic insights into how hemorrhage contributes to disease pathology not only in ROP, but also in other retinopathies with hemorrhage, such as DR, and identifies potential therapeutic targets.

2. Results

2.1. Hemorrhage correlates with retinal neovascularization

The Vermont Oxford Network (VON) database contained 370000 screened cases for ROP under 29 weeks' gestation in the last ten years. Both the rate of stage 3 ROP and the rate of ROP treatment were collected from the database and were given in percentage of the screened newborns broken down by year (Fig. 1a). The rate of stage 3 ROP has not changed in the last 10 years. The mean incidence of stage 3 ROP was 8.2 % with a range of 8.1–8.3 %. This shows that ROP disease is still present in routine neonatal practice. There has been a slight decrease in the rate of surgery for ROP over the last 10 years in this population, but it still accounts for more than 2 % of screened cases (Fig. 1a).

Vitreous hemorrhage can be present in stage 3 ROP [4]. However, its possible pathogenic role in the progression of ROP is not well understood.

To test our hypothesis on hemorrhage and its relationship to ROP severity, among our 824 stage 3 ROP cases for newborns under 1500 g birth weight we found 145 preterm infants with retinal hemorrhage and compared their data to 145 randomly selected preterm infants with no retinal hemorrhage. Differences in gestational age, birth weight, and the rate of laser therapy were examined for the two groups. Our results show no significant difference in gestational age (non-hemorrhaged 26.08 weeks vs. hemorrhaged 25.74 weeks) and birth weight (non-hemorrhaged 829.5 g vs hemorrhaged 800.3 g) between the hemorrhaged and non-hemorrhaged groups. In contrast, laser therapy was required for 26.8 % (39 of 145 patients) of premature infants with non-hemorrhaged retinas and 73.2 % (106 of 145 patients) of premature infants with hemorrhaged retinas (Fig. 1b). This shows that a significantly higher number of patients with hemorrhage required laser therapy compared to patients with non-hemorrhaged retinas.

We next examined the correlation between hemorrhage and activity of retinal neovascularization. To rule out the effect of the variability of neonatal intensive care unit (NICU) treatment, we selected 40 preterm infants from the hemorrhaged retina group, where one eye suffered hemorrhage during ROP screening and the other eye did not, and compared the extent of vasoproliferation in the two eyes. The mean gestational age of the patient group was 25.43 ± 0.22 weeks, and the birth weight was 780.0 ± 29.8 g. The degree of retinal vessel engorgement and tortuosity multiplied by "clock hours" served as the value for activity of neovascularization. The results showed that the rate of vasoproliferation was significantly higher in the hemorrhaged eye (3.87 ± 0.48 h) compared to the non-hemorrhaged eye of the same patient (1.22

a

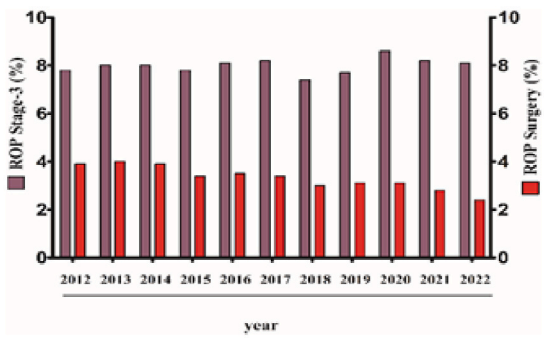

b

	Non-hemorrhaged patients	Hemorrhaged patients	*p*-value	*p*-value summary
Number (N)	145	145		
Gestation age (weeks)	26.08 ± 0.15	25.74 ± 0.14	0.4275	ns.
Birth weight (grams)	829.5 ± 20.05	800.3 ± 21.09	0.5443	ns.
Laser therapy	**39 (26.8 %)**	**106 (73.2%)**	**0.0002**	***

c

	Patients			
Gestation age (weeks)	25.43 ± 0.2261			
Birth weight (grams)	780.0 ± 29.82			
Number (eye pairs)	N=40			
Status	Non hemorrhaged	Hemorrhaged	*p*-value	*p*-value summary
Incipient proliferation (mean)	**1.225 ± 0.083**	**3.875 ± 0.487**	**<0.0001**	***

d

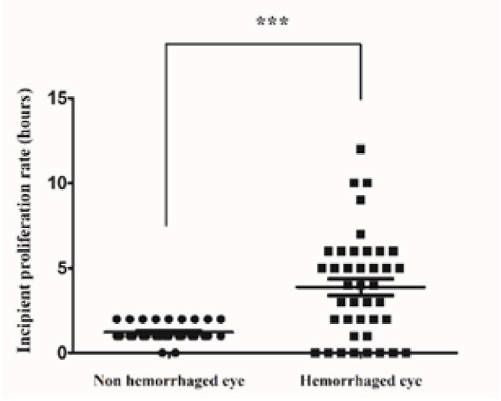

e

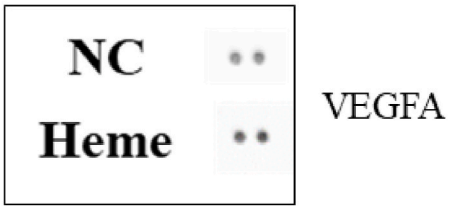

f

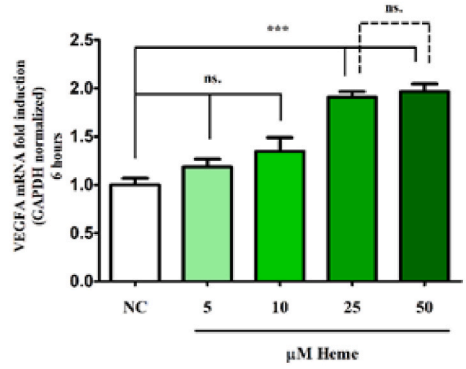

g

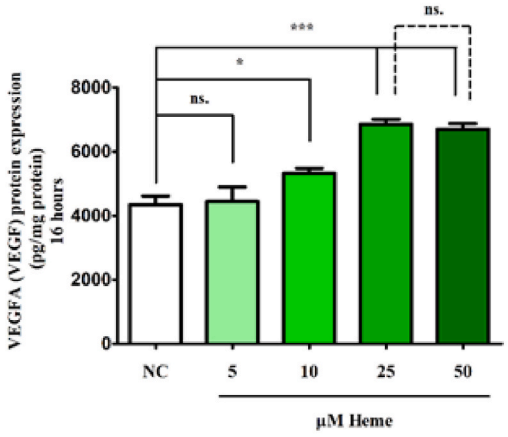

(caption on next page)

Fig. 1. Hemorrhage correlates with the incidence of severe ROP. **a** Incidence of ROP Stage-3 and ROP surgery in VON database 2012–2022. **b** Differences in gestational age, birth weight, and laser therapy between hemorrhage and non-hemorrhaged patients. N = 145 in both groups. Data are represented as mean value ± SEM. Statistical analysis was performed by one-way ANOVA test followed by Bonferroni correction. A value of $p < 0.05$ was considered significant. **c,d** Correlation between hemorrhage, gestational age, birth weight and vasoproliferation in the hemorrhaged group. N = 40. Data are represented as mean value ± SEM. Statistical analysis was performed by one-way ANOVA test followed by Bonferroni correction. A value of $p < 0.05$ was considered significant. **e** Human angiogenesis array analysis of cell culture supernatants of ARPE-19 cells exposed to heme (25 μM). Each group contained two replicates of culture supernatant mixtures. NC: non-treated cells. **f** Gene expression levels of VEGFA in ARPE-19 cells exposed to heme (5–50 μM). NC: non-treated cells. Data are represented as mean value ± SEM (n = 5). Statistical analysis was performed by one-way ANOVA test followed by Bonferroni correction. A value of $p < 0.05$ was considered significant. **g** VEGFA protein levels measured by ELISA in ARPE-19 cells exposed to heme (5–50 μM). NC: non-treated cells. Data are represented as mean value ± SEM (n = 5). Statistical analysis was performed by one-way ANOVA test followed by Bonferroni correction. A value of $p < 0.05$ was considered significant.

± 0.08 h) (Fig. 1c and d).

In conclusion, hemorrhage increases the frequency of the need for laser therapy and can be used as an indicator of severe ROP. What is more, in the same patient, hemorrhaged eyes exhibited increased vasoproliferation compared to non-hemorrhaged eyes emphasizing the strong correlation between the neovascularization and bleeding.

2.2. Heme induces VEGFA expression in human retinal pigment epithelial cells (ARPE-19 cells)

VEGFA expression, and consequently angiogenesis, are involved in the pathogenesis of ROP [6] and DR [28]. One of the well characterized in vitro cell culture model for VEGF synthesis and regulation is the human retinal pigment epithelial cell which is optimal for heme stress studies. To evaluate the relative levels of angiogenesis-related proteins, we performed a Human Angiogenesis Array on ARPE-19 cells cell supernatants. Supernatants of ARPE-19 cells cultures stimulated with heme (25 μM) were examined and compared to unstimulated cells. We showed that VEGFA was upregulated by heme in the cell culture supernatants (Fig. 1e).

To verify these results, we exposed ARPE-19 cells to various concentrations of heme (5–50 μM) and measured VEGFA mRNA expression by quantitative real-time PCR. We found that higher heme concentrations (25 and 50 μM) led to a ~ 2-fold increase in VEGFA gene expression compared to the control (Fig. 1f). At lower heme concentrations (5 and 10 μM), there was an upregulation of VEGFA gene expression, but this was not statistically significant (Fig. 1f). We then determined VEGFA protein levels in the cell culture supernatants by ELISA. We showed that heme (10, 25, and 50 μM) significantly induced VEGFA protein expression (Fig. 1g). The release of VEGFA was comparable at the higher doses of heme (25 and 50 μM) (Fig. 1g).

Determination of cell viability of ARPE-19 cells in response to heme was critical for our cell culture experiments, since we wanted to avoid a near retinal pigment epithelial death phenomenon and studies. Next, we analyzed whether heme induces cell death in ARPE-19 cells. Cells were treated with various doses of heme (10–300 μM) for 6 and 16 h, then cell viability was tested by MTT assay (Supplementary figure). Our data showed that heme did not trigger cell death in ARPE-19 in the concentration range tested.

Taken together, it can be concluded that heme induces the expression of VEGFA in ARPE-19 cells in a dose-dependent manner.

2.3. Heme induces endothelial tube formation in HUVEC cultures

To investigate whether heme induces endothelial tube formation in HUVEC cultures, a tube formation assay was performed as described in the Methods section. Our results showed that conditioned media from ARPE-19 cells exposed to heme markedly induced tube formation in HUVEC cultures on Geltrex LDEV-Free Reduced Growth Factor Basement Membrane Matrix compared to that collected from untreated ARPE-19 cells when concentrated to 10-fold or 25-fold (Fig. 2). This indicate that heme amplifies the angiogenic potential of ARPE-19 cell cultures.

2.4. RNA sequencing transcriptomic signatures in ARPE-19 cells upon heme exposure

To begin to understand the underlying mechanism by which hemorrhage increases neovascularization, we performed RNA-seq on ARPE-19 cells treated with heme (25 μM) and compared to untreated cells. This analysis revealed 370 differentially expressed genes (DEGs) that met our inclusion criteria for fold change expression (>1.5) in heme-stimulated ARPEs relative to control. The heme-stimulated and control groups were clearly separated in the heatmap (Fig. 3a). Volcano plot showed that MIR6720, TFRC, PDIA4, HYOU1, and HSPA5 were the most downregulated genes, while SAT1, IFUTM10, CHAC1, PFKFB4, and HMOX1 were the most upregulated genes (Fig. 3b).

To identify the function of the DEGs, multiple bioinformatics analyses were performed using the Cytoscape ClueGO bioinformatics tool [29]. We showed that overrepresented GOterms in heme-stimulated ARPE-19 cells were mostly involved in biological processes related to DNA replication, cell cycle checkpoint, cholesterol biosynthesis, positive regulation of angiogenesis, regulation of transcription from RNA polymerase II promoter in response to stress, telomere maintenance, and cellular response to unfolded protein (Fig. 3c).

Among genes annotated to the positive regulation of angiogenesis, 13 genes (6.95 per cent of annotated to the positive regulation of angiogenesis) showed significant change in response to heme. Out of these, 11 significantly increased (ADM, ADM2, ANGPTL4, BTG1, CYP1B1, HIPK2, HK2, HMOX1, KLF4, RHOB, VEGFAA), and 2 (CXCL8, THBS1) significantly decreased in heme-stimulated ARPE-19 cells (Fig. 3d).

Next, we examined the relative changes in genes involved in lipid metabolism and biosynthetic pathways. We showed that 25 genes involved in this process were significantly upregulated, while two genes (MFSD2A, P2RY6) were down-regulated in heme-stimulated ARPE-19 cells (Fig. 3e).

To explore the relationship between DEGs in lipid biosynthesis and positive regulators of angiogenesis pathways, ClueGO plug-in was used to perform GO functional enrichment in Cytoscape software. The results indicated that the DEGs were significantly enriched in cholesterol biosynthetic process, regulation of alcohol biosynthetic process, cholesterol metabolic process, regulation of steroid metabolic process, and regulation of lipid biosynthetic process (Fig. 3f).

These results indicate the dynamic induction of positive regulators of angiogenesis and lipid biosynthetic processes in response to heme, which may underline the importance of the role of retinal hemorrhage in retinal pathophysiology.

2.5. Heme induces nuclear translocation of HIF-1α and Activates HIF-regulated gene expression in ARPE-19 cells

Since anti-VEGFA therapy of ROP in the second phase of the disease is very effective in saving vision contrary to the failing preventive efficiency of IGF-1 supplementation during the first phase, the importance of the mainly hypoxia inducible factor-1 α (HIF-1α)-regulated VEGFA should be our focus in hemorrhage/heme modified retinal pigment epithelium (RPE) function. Hypoxia and hypoxia inducible factors are important inducers of VEGFA production [30]. First, we analyzed the

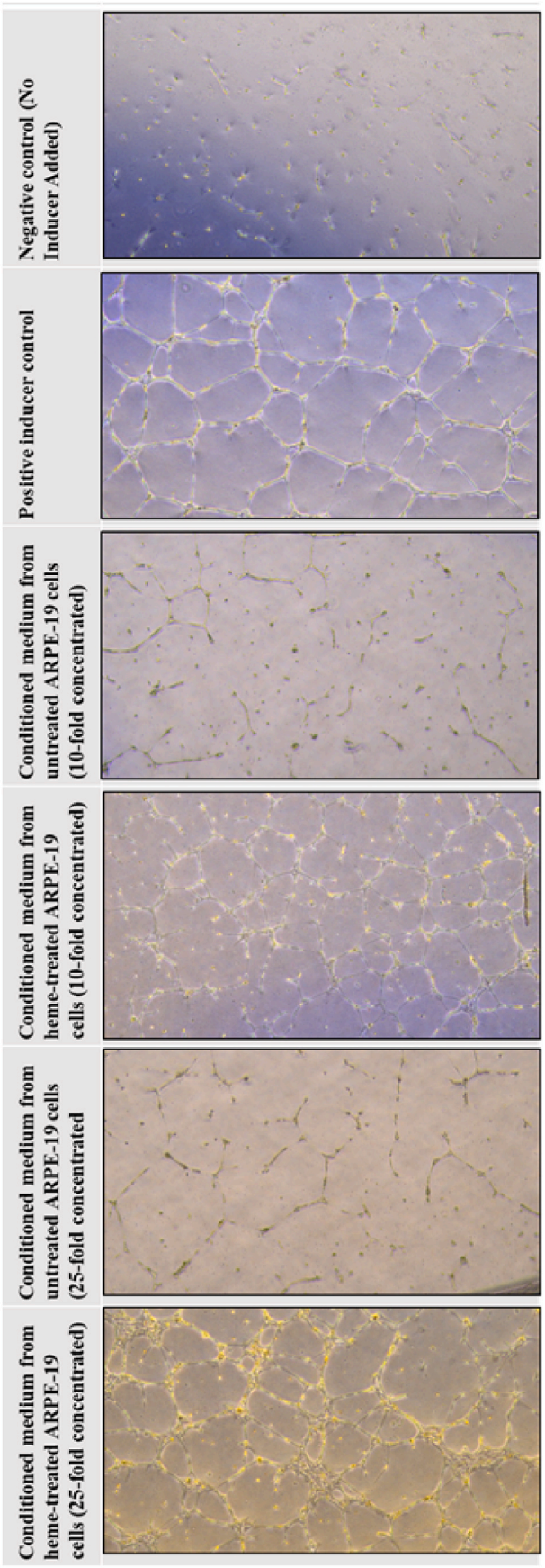

(caption on next column)

Fig. 2. Endothelial Cell Tube Formation Assay. HUVEC cultures were plated on Geltrex LDEV-Free Reduced Growth Factor Basement Membrane Matrix and exposed to 10-fold or 25-fold concentrated ARPE-19 cell culture supernatants from heme-exposed cells. For positive inducer control of tube formation, HUVECs exposed to Medium 200 supplemented with Large VesseI Endothelial Supplement (LVES), while for negative control, HUVECs exposed to Medium 200 without LVES were used (n = 3). Tube formation was observed using Leica DMi1 microscope.

nuclear translocation of HIF-1α by treating ARPE-19 cells with heme (5–25 μM) to determine whether HIF-1α is directly involved in heme-induced VEGFA production. Immunofluorescence analysis showed a robust increase in HIF-1α nuclear translocation upon exposure of ARPE-19 cells to heme (Fig. 4a). To extend our findings, we investigated how heme affects the gene expression of two hypoxia-regulated genes, Glucose transporter 1 (GLUT1) [31] and Pyruvate dehydrogenase kinase 1 (PDK1) [32], both of which have been implicated in the pathology of DR and ROP [33,34]. Our results showed that both GLUT1 and PDK1 expressions were upregulated ~2-fold in ARPE-19 cells exposed to heme (Fig. 4b and c). Next, we measured the lactate concentration in the supernatants of ARPE-19 cells cultures exposed to heme (5–50 μM). Lactate levels were significantly elevated in response to heme (Fig. 4d).

In summary, heme enhances nuclear translocation of HIF-1α, activates HIF-regulated gene expression, and increases lactate production in ARPE-19 cells.

2.6. Inhibition of HO-1 does not aggravate heme-induced VEGFA production in ARPE-19 cells

HO-1 is the main catabolic enzyme of heme, and HO-1 expression plays a key role in VEGFA induction in several cell types [35,36]. Furthermore, the HO-1 inhibitor tin protoporphyrin IX (SnPPIX) inhibits HO-1-dependent VEGFA production [35,37,38]. We then investigated whether inhibition of HO-1 by SnPPIX attenuates heme-induced VEGFA production in ARPE-19 cells. Our experiments showed that SnPPIX had no effect on heme-induced VEGFA gene (Fig. 5a) or protein (Fig. 5b) expression. To further confirm this finding, we next examined whether SnPPIX affects GLUT1 and PDK1 levels in ARPE-19 cells exposed to heme. Our results showed that SnPPIX had no effect on the heme-induced expression of GLUT1 and PDK1 in heme-treated ARPE-19 cells (Fig. 5c and d). To verify these results, we knocked down HO-1 expression using small interfering RNA. We showed that knockdown of HO-1 expression did not affect heme-induced VEGFA production in ARPE-19 in the concentration range (5–50 μM) tested (Fig. 5e and f).

To test whether scavenging heme with the specific heme-binding protein A1M, we co-incubated heme with A1M followed by the measurement of VEGFA mRNA after 6 h. Our results showed that scavenging free heme with rA1M prevents heme-induced VEGF expression (Fig. 5g). Based on these data, we are convinced that the end-products of heme catabolism by HO-1 are not necessary for VEGFA induction in our case.

2.7. TLR4 is not connected to VEGF production in response of ARPE-19 to heme

Toll-like receptors, including Toll-like receptor 4 (TLR4), are expressed in ARPE-19 cells [39]. TLR4 signaling is implicated in pathogenesis of DR [40], and the TLR4 inhibitor TAK-242 attenuates aberrant angiogenesis in oxygen-induced retinopathy (OIR) model [41]. Given that heme could activate TLR4 signaling [42], we next asked whether inhibiting TLR4 signaling with TAK242, a specific inhibitor of TLR4 signaling, could inhibit heme-induced hypoxic response and VEGF induction in ARPE-19 cells. We found that TAK242 did not inhibit heme-induced VEGF expression (Fig. 6a and b). Consistent with this, TAK242 had no effect on either GLUT1 or PDK1 mRNA expression (Fig. 6c and d). Thus, our results show that TLR4 signaling is unlikely to

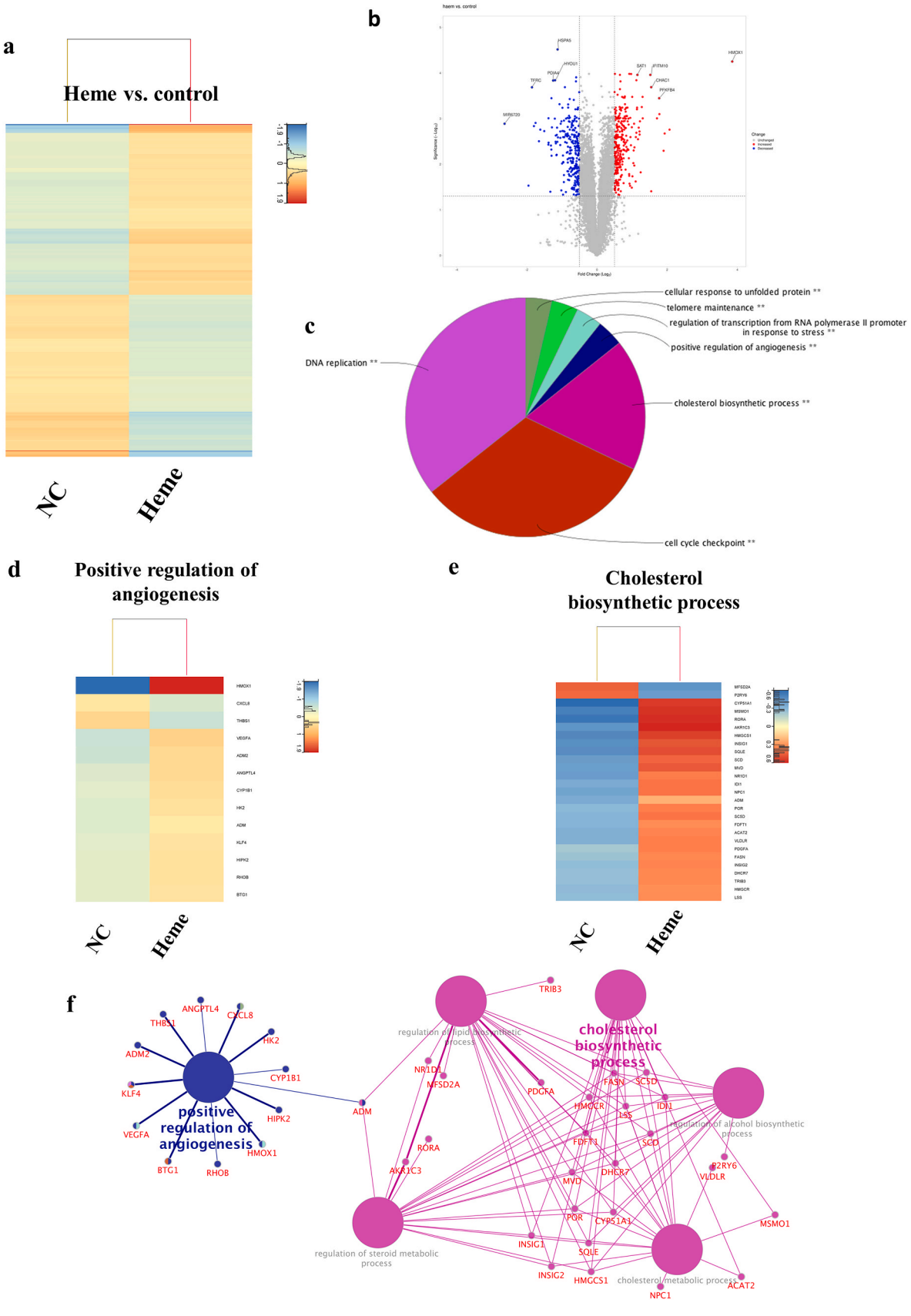

(caption on next page)

Fig. 3. RNA sequencing transcriptomic signatures in ARPE-19 cells upon heme exposure. **a** Heatmap representation of the differentially expressed genes identified in RPEs exposed to heme (25 μM) compared to the control (n = 3). NC: non-treated cells. The color key represents gene expression levels with darker colors representing higher (red) or lower (blue) gene expression. **b** Volcano plot analysis of the differentially expressed genes identified in RPEs exposed to heme (25 μM) compared to the control. **c** Overrepresented GOterms in heme-stimulated RPEs compared to controls using the Cytoscape ClueGO bioinformatics tool. **d** RNA sequencing analysis of the positive regulators of angiogenesis and **e** cholesterol biosynthetic process in heme-stimulated ARPE-19 cells compared to controls. Raw sequencing data (fastq) was aligned to human reference genome version GRCh38 using HISAT2 algorithm and BAM files were generated. Downstream analysis was performed using StrandNGS software (www.strand-ngs.com). BAM files were imported into the software DESeq algorithm was used for normalization. Moderated T-test was used to determine differentially expressed genes between conditions, p value < 0.05 was considered significant difference. **f** GO functional enrichment analysis of the positive regulators of angiogenesis and e cholesterol biosynthetic process in heme-stimulated ARPE-19 cells compared to controls using the Cytoscape software.

be involved in heme-induced hypoxic transition and VEGF production in ARPE-19 cells.

2.8. Heme induces VEGFA production via PI3K/Akt pathway in ARPE-19 cells

HIF-1α can be induced by various growth factors and cytokines through the phosphoinositide 3-kinase-AKT- Mammalian target of rapamycin (PI3K-AKT-mTOR) pathway in an oxygen-independent manner [43–45]. Furthermore, the PI3K-AKT-mTOR pathway has a key role in numerous cellular functions, including angiogenesis [46]. Phosphorylation of Ser473 required for AKT activation [47]. Therefore, we next sought to identify whether heme induces the phosphorylation of Ser473. Immunoblot analysis of ARPE-19 cells exposed to heme revealed that heme increased the phosphorylation Ser473 compared to untreated cells without affecting the total level of AKT (Fig. 7a). This was also verified by immunofluorescent analysis of heme-treated cells (Fig. 7b). Having shown that AKT phosphorylation is induced by heme, we next asked whether PI3K inhibition could reduce heme-induced VEGFA production and hypoxic response. For this reason, we exposed the ARPE-19 cells to LY294002, a potent inhibitor of PI3K [48], before pulsing them with heme. We showed that LY294002 attenuated VEGFA expression and secretion in ARPE-19 cells exposed to heme (Fig. 7c and d). Consistently, LY294002 significantly reduced GLUT1 and PDK1 expressions in ARPE-19 cells treated with heme (Fig. 7e and f). This suggests that inhibiting PI3K signaling may have anti-angiogenic potential in hemorrhagic retinopathies.

2.9. HIF-1α inhibitor BAY 87–2243 and mTOR inhibitor rapamycin reduce heme-induced VEGFA production in ARPE-19 cells

To determine whether pharmacological inhibition of HIF-1α could reduce the heme-induced hypoxic response, we evaluated VEGFA, GLUT1, and PDK1 expression in heme-exposed ARPE-19 cells treated with a specific HIF-1α inhibitor, BAY 87–2243. We showed that VEGFA mRNA expression (Fig. 8a) and protein secretion (Fig. 8b) were reduced by treatment of ARPE-19 cells with the HIF inhibitor BAY 87–2243 in a dose dependent manner. Next, we examined how BAY 87–2243 could affect GLUT1 and PDK1 expressions. We showed that BAY 87–2243 dose-dependently decreased the levels of both GLUT1 (Fig. 8c) and PDK1 (Fig. 8d). Collectively, these results suggest that pharmacological inhibition of HIF-1α could reduce the heme-induced hypoxic response and VEGFA production in ARPE-19 cells.

Rapamycin has been shown to reduce VEGFA expression in vitro in ARPE-19 cells [49]. However, how rapamycin affects heme-induced hypoxic gene expression and VEGFA production remains incompletely characterized. Therefore, we performed qPCR analysis on ARPE-19 cells treated with rapamycin and heme in comparison to heme-treated ARPE-19 cells alone. Our results showed that rapamycin down-regulated heme-induced VEGFA expression and VEGFA protein secretion (Fig. 8e and f). In parallel, we also observed a significant decrease in both GLUT1 and PDK1 levels in response to rapamycin in heme-treated ARPE-19 cells (Fig. 8g and h), suggesting that targeting mTOR may be an effective intervention to inhibit both VEGFA production and hypoxic reprogramming after hemorrhage.

2.10. ER stress is not involved in VEGFA production in ARPE-19 cells upon heme exposure

Inhibition of the protein kinase R-like endoplasmic reticulum kinase (PERK) arm of endoplasmic reticulum (ER) stress signaling reduces both C/EBP homologous protein (CHOP) and VEGFA expression in ARPE-19 cells [50]. This raised the question of whether the PERK/CHOP arm of ER stress is involved in the heme-induced production of VEGFA in the ARPE-19 cells. Therefore, we exposed ARPE-19 cells to the selective PERK inhibitor GSK2656157 in the presence of heme and compared the expression of CHOP and VEGFA with that of ARPE-19 cells exposed to heme alone. We showed that heme induced a 3-fold induction of CHOP expression, which was significantly inhibited by the PERK inhibitor GSK2656157 (Fig. 9a). We then quantified VEGFA mRNA expression and protein secretion in the presence of heme and the PERK inhibitor GSK2656157. Our results showed that PERK inhibition did not decrease but slightly increased heme-induced VEGFA expression (Fig. 9b and c). Next, we evaluated the effects of GSK2656157 on GLUT1 and PDK1 expressions. Our results showed that GSK2656157 did not affect heme-induced GLUT1 and PDK1 expressions (Fig. 9d and e), suggesting that heme-induced hypoxic response is not related to heme-induced ER stress and CHOP expression. These results suggest that the heme-induced hypoxic response and the expression of VEGFA are independent of the PERK/CHOP axis.

2.11. Heme reduces oxidative phosphorylation and induces a glycolytic response in ARPE-19 cells

Mitochondrial damage is involved in retinopathies [51,52]. Our ARPE-19 cell culture data revealed that heme induced VEGFA through the HIF-1α pathway. This observation highlights a possible mitochondrial heme effect in this model. To investigate the significance of alterations in mitochondrial function in response to heme, we analyzed the mitochondrial oxygen consumption rate in ARPE-19 cells exposed to heme and in the presence of absence of BAY 87–2243, LY294002, and rapamycin. Basal respiration, maximal respiration, spare respiratory capacity, and ATP production were significantly decreased in heme-stimulated ARPE-19 cells (Fig. 10a–e). These were further decreased by BAY 87–2243 and LY294002 but not by rapamycin (Fig. 10a–e).

The glycolytic function of ARPE-19 cells in response to heme and the different inhibitors were measured using the glycolysis stress test (Fig. 10f–i). The rate of glycolysis was significantly increased by heme (Fig. 10g). This rate was further aggravated by both BAY 87–2243 and LY294002 (Fig. 10g). Rapamycin significantly decreased the rate of glycolysis in heme-stimulated cells (Fig. 10g). Next, we measured glycolytic capacity that showed no significant differences between the different groups (Fig. 10h). Glycolytic reserve was significantly decreased by heme between 5 and 25 μmol/L but not by the highest heme dose (50 μmol/L) (Fig. 10i). Glycolytic reserve was significantly decreased by both BAY 87–2243 and LY294002, and a lesser extent, but still significantly by rapamycin (Fig. 10i).

Heme is known as cellular alarmin with several metabolic consequences, one of them is sensitization towards active oxygen species. Heme itself may generate free radicals or increases cellular free radical concentration if the mitochondrial function is disturbed. We studied the

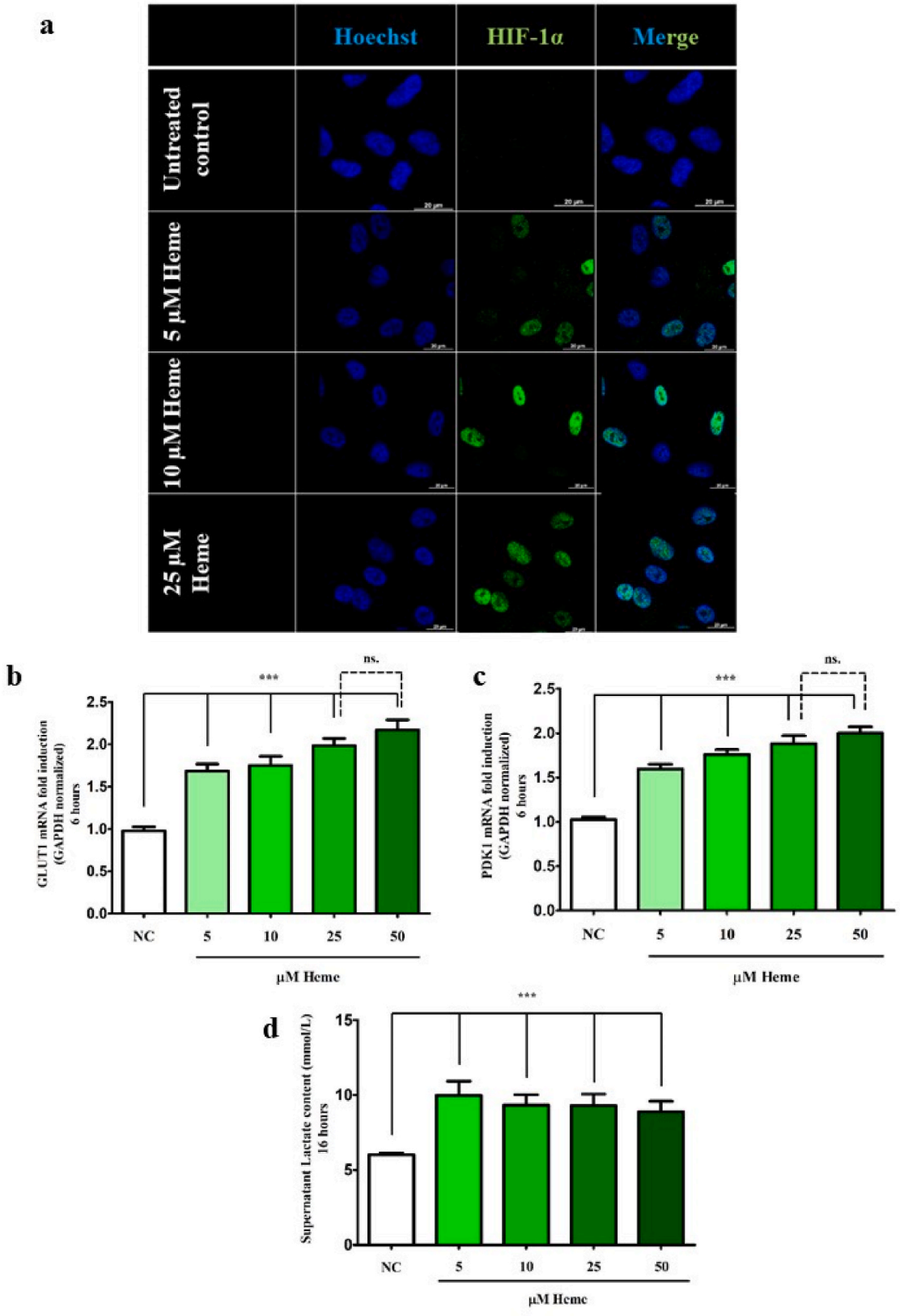

Fig. 4. Heme Induces Nuclear Translocation of HIF-1α and Activates HIF-Regulated Gene Expression in ARPE-19 cells. **a** Immunofluorescent analysis of HIF-1α nuclear translocation in ARPE-19 cells exposed to heme (5–25 μM) compared to non-treated control. Nuclei are visualized with Hoechst staining (n = 3). **b** Gene expression levels of GLUT1 and **c** PDK1 in ARPE-19 cells exposed to heme (5–50 μM). **d** Lactate concentration in the supernatants of ARPE-19 cells exposed to heme (5–50 μM). NC: non-treated cells. Data are represented as mean value ± SEM. Statistical analysis was performed by one-way ANOVA test followed by Bonferroni correction.

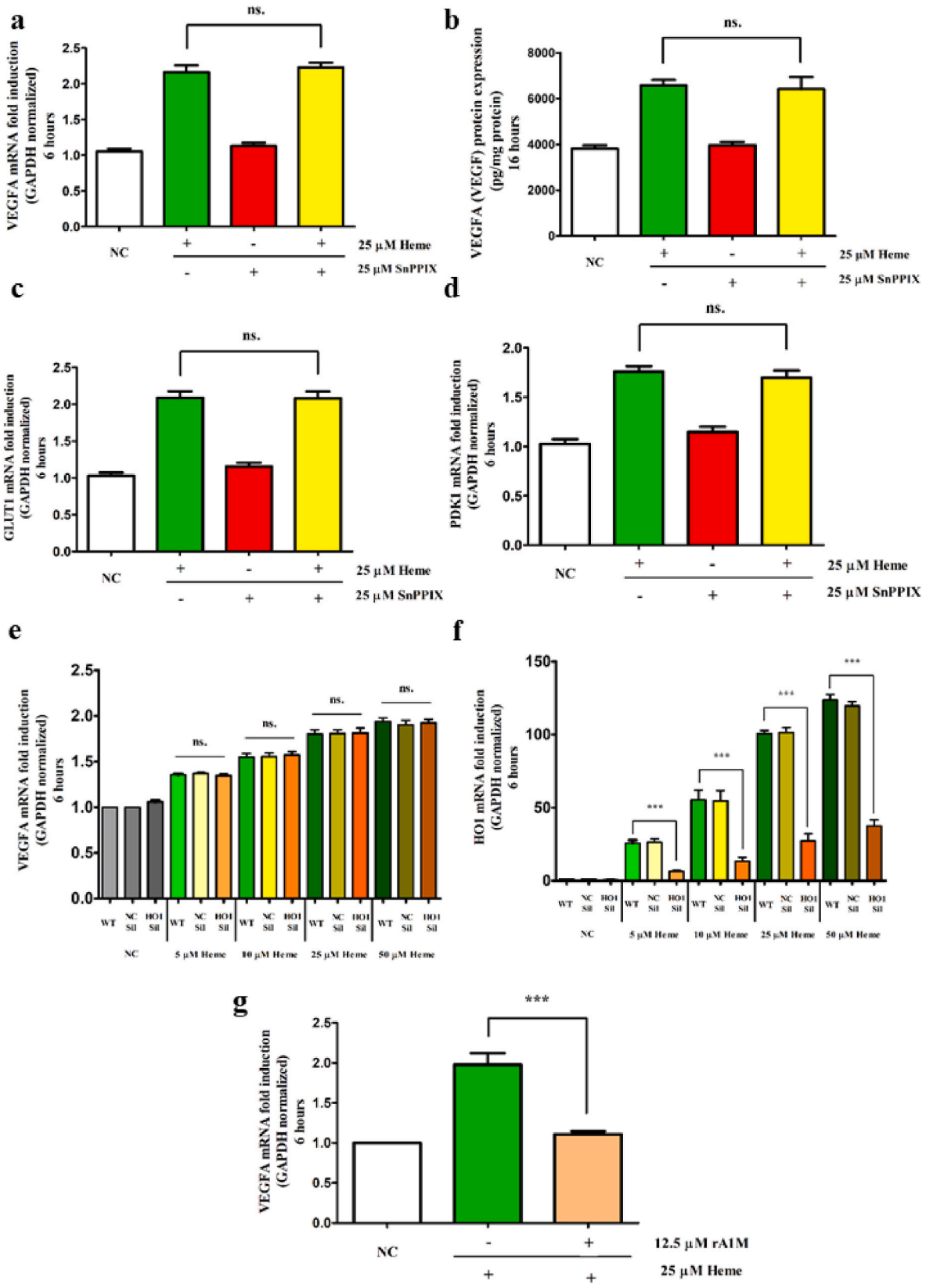

Fig. 5. Inhibition of HO-1 does not aggravate heme-induced VEGFA production in ARPE-19 cells. **a** Gene expression and **b** VEGFA protein levels measured by ELISA in ARPE-19 cells exposed to heme (25 μM) and SnPPIX (25 μM). **c** Gene expression levels of GLUT1 and **d** PDK1 in ARPE-19 cells to heme (25 μM) and SnPPIX (25 μM). **e** Gene expression levels of VEGFA and **f** HO-1 in HO-1-silenced ARPE-19 cells exposed to heme (5–50 μM). **g** Gene expression levels of VEGFA in ARPE-19 cells exposed to heme (25 μM) alone or in complex with A1M (12.5 μM) NC: non-treated cells; A1M: alpha-1-microglobulin. Data are represented as mean value ± SEM (n = 3). NC: non-treated cells Statistical analysis was performed by one-way ANOVA test followed by Bonferroni correction. A value of $p < 0.05$ was considered significant.

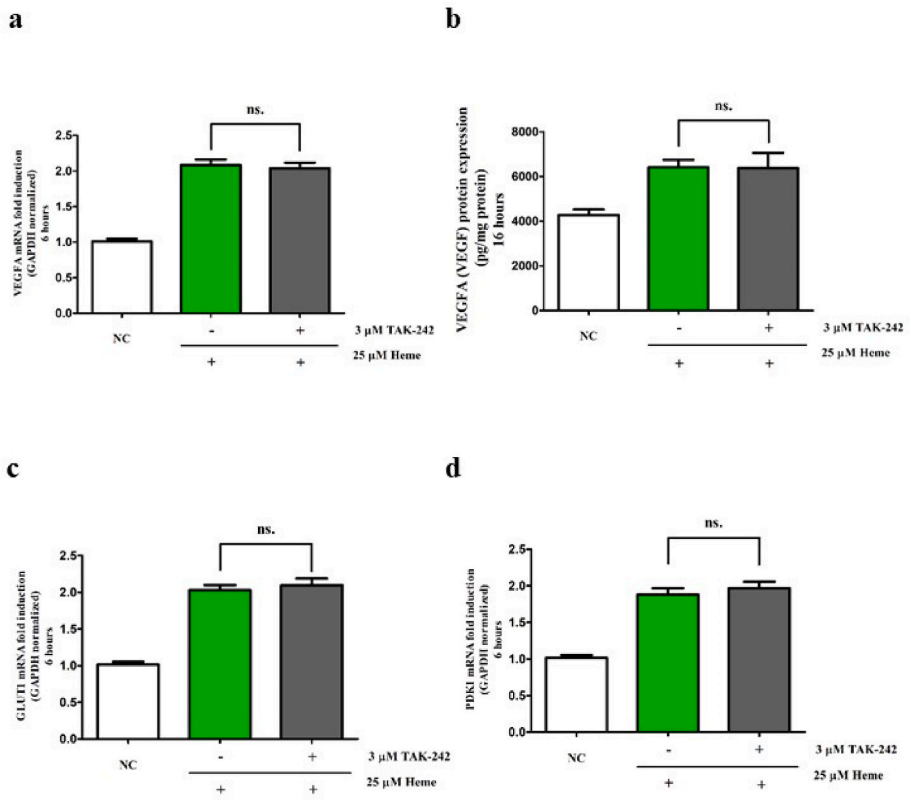

Fig. 6. TLR4 is not connected to heme-induced VEGF production in ARPE-19 cells. **a** VEGF gene expression and **b** protein levels in ARPE-19 cells exposed to heme (25 μM) and TAK-242 (3 μM). **c** Gene expression levels of GLUT1 and **d** PDK1 in ARPE-19 cells exposed to heme (25 μM) and TAK-242. NC: non-treated cells, TLR4: Toll-like receptor 4 (n = 3). Statistical analysis was performed by one-way ANOVA test followed by Bonferroni correction. A value of $p < 0.05$ was considered significant.

probable cellular free radical generation by heme through the transcriptomic changes of antioxidant enzymes mRNAs and by direct measurement of cellular oxygen species after ARPE-19 cell heme treatment.

DEGs involved in antioxidant response which significantly changed ($p < 0.05$) are depicted in Fig. 11a. Importantly, DEGs that met our inclusion criteria for fold change expression (>1.5) in heme-stimulated ARPEs relative to control only include two DEGs, those are glutathione-disulfide reductase (GSR) and sulfiredoxin 1 (SRXN1). Both GSR and SRXN1 were upregulated by heme. Other components of the antioxidant response such as superoxide dismutase 2, mitochondrial (SOD2), glutathione synthetase (GSS), glutathione S-transferase C-terminal domain containing (GSTCD), thioredoxin 2 (TXN2), thioredoxin reductase 3 (TXNRD3), and peroxiredoxin 6 (PRDX6) were significantly downregulated, while. Glutathione S-transferase mu 3 (GSTM3), microsomal glutathione S-transferase 1 (MGST1), glutathione-disulfide reductase (GSR), microsomal glutathione S-transferase 3 (MGST3), glutathione peroxidase 3 (GPX3), thioredoxin (TXN), thioredoxin reductase 1 (TXNRD1), and peroxiredoxin 1 (PRDX1) were significantly upregulated by heme with fold change expression <1.5. Then, we examined oxidative stress using CellRox staining in cells exposed to heme. We found that heme did not induce detectable oxidative stress in ARPE-19 cells compared to untreated cells (Fig. 11b). However, menadione, a well-known inducer of oxidative stress, markedly induced reactive oxygen species generation. To detect whether heme induces lipid peroxidation in ARPE-19 cells, cells were exposed to heme and lipid peroxidation was measured with Image-iT Lipid Peroxidation Kit as described in the Methods section. The signals were then quantitated and the ratios of the signal from red to green channels were used to quantify lipid peroxidation in cells according to the manufacturer's guide. In control cells, most of the signal is in red channel and the ratio of red/green was high and when the cells are treated with menadione, the ratios are markedly significantly lower. In heme-treated cells, the signal is in red channel and the ratio of red/green comparable with those detected in the untreated control cells (Fig. 11c and d) suggesting that heme did not trigger lipid peroxidation under our experimental conditions.

Since heme treatment of ARPE-19 cells resulted in significant mitochondrial functional consequences, we visualized mitochondria by fluorescent nanoscopy. In order to evaluate the effect of heme on mitochondria, we stained ARPE-19 cells with Mitotracker Red probe that accumulates in the mitochondria of live cells and observed mitochondria using confocal microscopy. Our results showed that heme (25 μmol/L) led to the aggregation of mitochondria that was mitigated by rapamycin (Fig. 12a). BAY 87–2243 alone or in combination with heme tremendously decreased the accumulation of Mitotracker Red in the mitochondria (Fig. 12a). To quantify these, ten individual Region of interest (ROIs) (1 μm^2) were quantified. Quantification of ROIs supported our findings (Fig. 12b).

We showed heme induced the aggregation of mitochondria, decreased oxidative phosphorylation, provoked a glycolytic response, but not induced oxidative stress in ARPE-19 cells.

2.12. Hemoglobins (Hbs) induce VEGF, PDK-1, and GLUT-1 expressions in ARPE-19 cells

Evidence shows that hemolysis products, specifically Hb itself, have profound effects on angiogenesis. Hb induces VEGF secretion in tumor cells [53]. Therefore, we examined VEGFA in response to Hbs. For control, heme (25 μM) was used. Our results showed that OxyHb, MetHb as well as FerrylHb significantly induced VEGFA expression that was comparable or even higher than that detected in heme-exposed cells (Fig. 13a). All Hbs and heme significantly induced HO-1 (Fig. 13b),

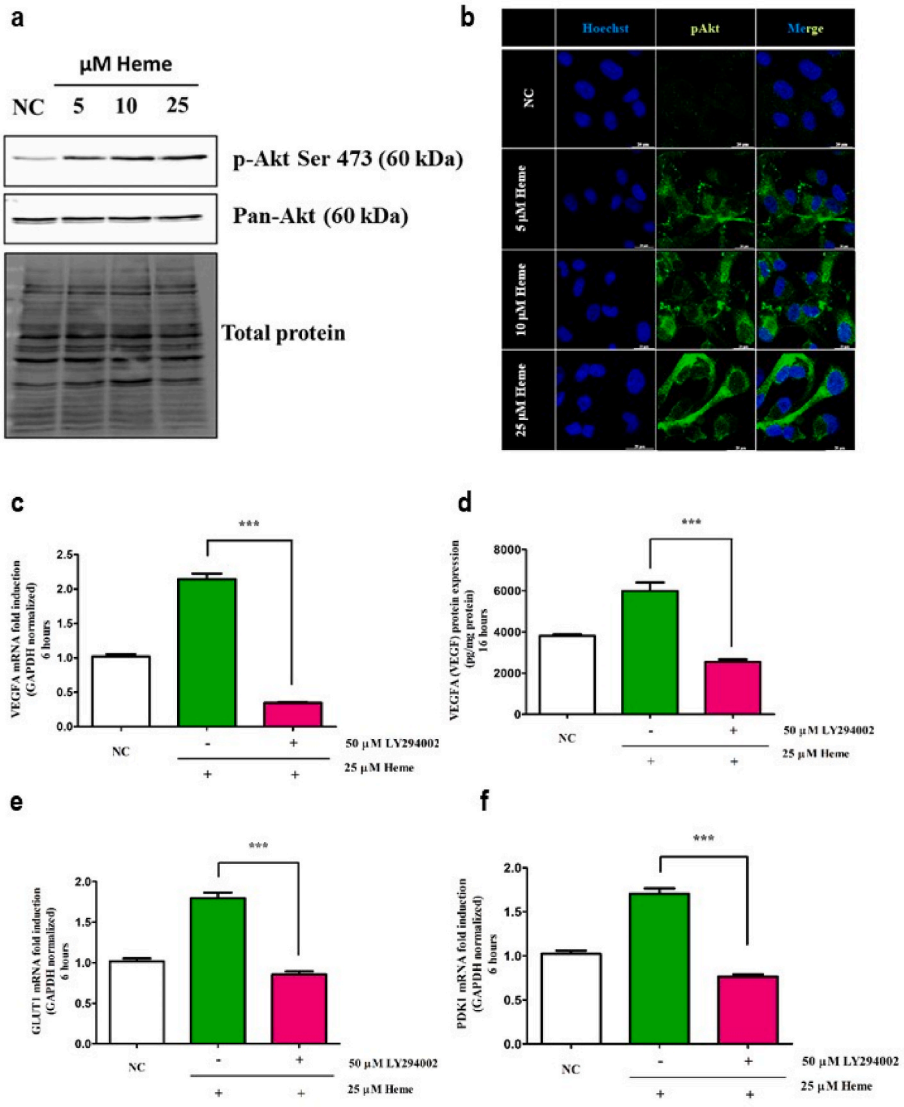

Fig. 7. Heme induces VEGFA production via PI3K/Akt pathway in ARPE-19 cells. **a** Immunoblot analysis of Akt (Ser 473) phosphorylation in response to heme (5–25 μM, n = 3). Immunoblots are cropped from different parts of the same gel. Uncropped immunoblots are presented in the Supplementary information. **b** Immunofluorescent analysis of Akt (Ser 473) phosphorylation in response to heme (5–25 μM; n = 3). **c** Gene expression and **d** VEGFA protein levels in ARPE-19 cells exposed to heme (25 μM) and LY294002. e Gene expression levels of GLUT1 and **f** PDK1 in ARPE-19 cells exposed to heme (25 μM) and LY294002. NC: non-treated cells. Data are represented as mean value ± SEM (n = 6). Statistical analysis was performed by one-way ANOVA test followed by Bonferroni correction. A value of $p < 0.05$ was considered significant.

GLUT-1 (Fig. 13c), and PDK-1 (Fig. 13d) expressions. These results suggest that Hbs, similar to heme, effectively induce VEGFA and GLUT1 as well as PDK1 expression.

Next, we measured the extent of Hb oxidation catalyzed by ARPE-19 cells. The oxidation process of Hb was followed by measuring the oxidation states of the heme-iron. The quantity of the oxidation forms of iron was determined spectrophotometrically, as summarized in the Methods section. Analysis of absorption spectra (Fig. 13e) and the quantification of the oxidation forms of iron showed that Hb is readily oxidizing in ARPE-19 cell culture supernatants (Fig. 13f). This was also demonstrated by immunoblotting that detected cross-linked Hb as a marker of Hb oxidation (Fig. 13g).

3. Discussion

In ROP, which is one of the best characterized retinal vascular diseases, we described increased retinal neovascularization in premature newborns when hemorrhage was observed during their ROP screening. Based on our transcriptomic, proteomic and signal transduction results, we can define that heme was capable to stimulate angiogenic factors by ARPE-19 cells. This heme-stimulated proangiogenic profile switch of ARPE-19 cells may suggest that heme is one of the ultimate mediators in hemorrhage-induced neovascularization contributing to the enhanced proangiogenic status of the retina. This clinical and in vitro cellular model strengthens our hypothesis, that bleeding is not an innocent bystander of retinal pathologies, moreover it is one of the risk factors of retinal vasculopathies.

We observed that preterm infants with retinal hemorrhage required laser therapy more frequently than those without retinal hemorrhage. In addition, in the retinal hemorrhage group, there was a significant increase in the activity of neovascularization in the eye with retinal hemorrhage in comparison to the eye without retinal hemorrhage in the same patient. These results are in good agreement with other studies concluded that vitreous hemorrhage is not only a marker for advanced ROP, but also an additional risk factor for a poor outcome [54]. Our clinical observation supports earlier study on ROP complicated with

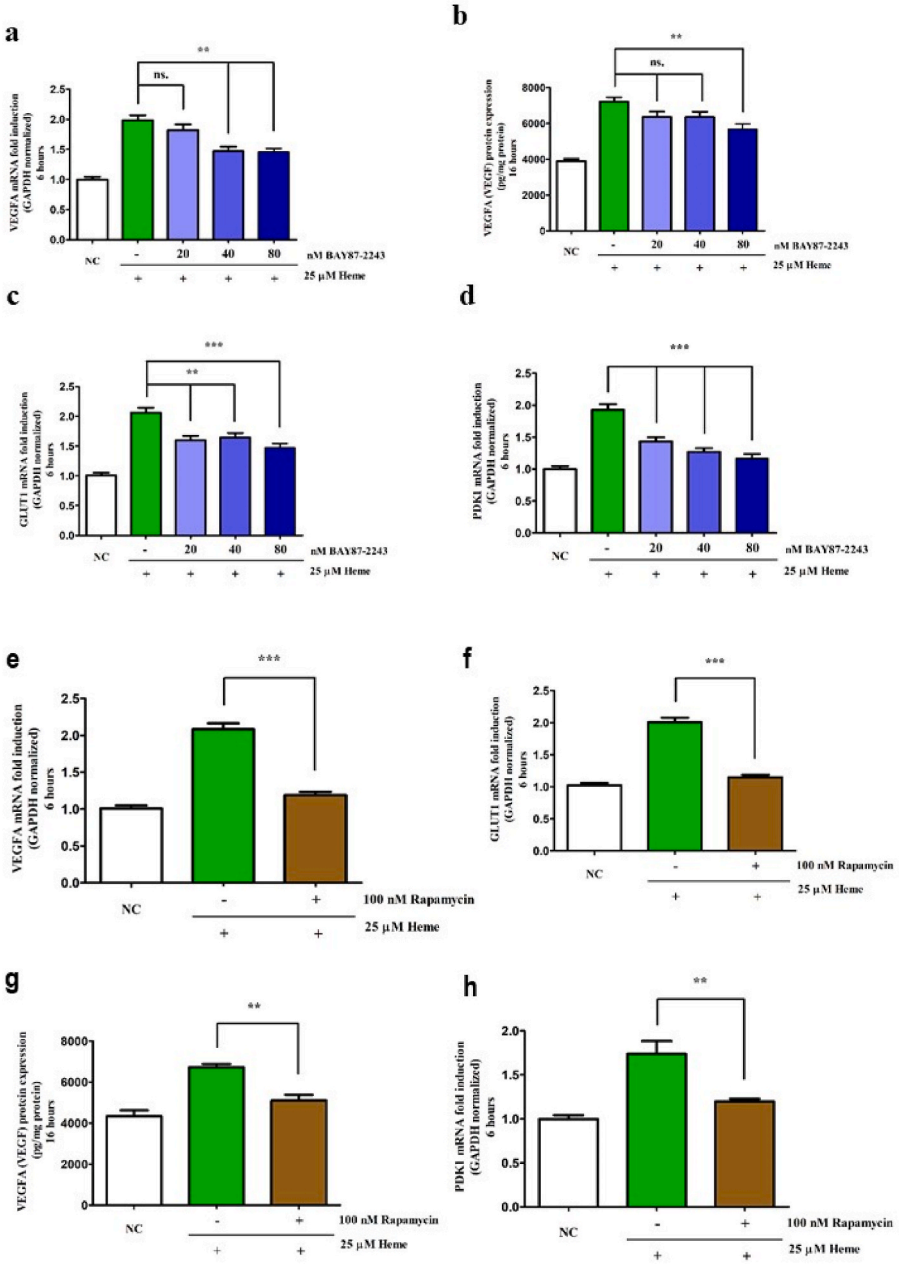

Fig. 8. HIF-1α inhibitor BAY 87–2243 and mTOR inhibitor rapamycin reduce heme-induced VEGFA production in ARPE-19 cells. **a** VEGFA gene expression and **b** protein levels in ARPE-19 cells exposed to heme (25 μM) and BAY 87–2243 (20–80 nM). **c** Gene expression levels of GLUT1 and **d** PDK1 in ARPE-19 cells exposed to heme (25 μM) and BAY 87–2243 (20–80 nM). NC: non-treated cells. **e** VEGFA gene expression and **f** protein levels in ARPE-19 cells exposed to heme (25 μM) and Rapamycin (100 nM). **g** Gene expression levels of GLUT1 and **h** PDK1 in ARPE-19 cells exposed to heme (25 μM) and Rapamycin. NC: non-treated cells. Data are represented as mean value ± SEM (n = 6). Statistical analysis was performed by one-way ANOVA test followed by Bonferroni correction. A value of $p < 0.05$ was considered significant.

retinal bleeding where the proportion of premature newborns receiving treatment was also higher than that of in the non-hemorrhaged group, 68.3 % vs. 43.4 %, although in their cohorts the gestational age and birth weight of the retinal hemorrhage group were lower than those of the non-hemorrhagic group [4]. Future studies are needed to provide more information on the association between bleeding and ROP.

Retinal pigment epithelial cells are major contributors to the retinal secretome involved in retinal pathologies [55]. Here we showed that gene expression profile of heme-treated ARPE-19 cells and vitreous markers of retinopathy in ROP and DR patients or in hyperoxia-induced animal ROP models showed high overlap, indicating that the similar expression patterns could already suggest the pathophysiological involvement of hemorrhage/heme in these retinopathies. Increased expression of Retinoic-acid-receptor-related orphan receptor alpha (RORA) [56], VEGFA [6], angiopoietin-like protein 4 (ANGPTL4) [57], are detected in ROP and DR patients, and these genes were upregulated in ARPE-19 cells exposed to heme. Thrombospondin-1 (THBS1) was also markedly down-regulated by heme in ARPE-19 cells, which is consistent with a report showing that THBS1 deficiency aggravates the pathogenesis of DR [58]. Similarly, heme also decreased the expression of major facilitator superfamily domain-containing 2a (MFSD2A) which protein is reported to alleviate vascular dysfunction in retinopathies [59]. In contrast to these, C-X-C Motif Chemokine Ligand 8 (CXCL8) which is up-regulated in retinopathies [60], was decreased in ARPE-19 cells in response to heme. Levels of several genes involved in angiogenesis, such as 6-phosphofructo-2-kinase/fructose-2, 6-bisphosphatase 4 (PFKFB4)

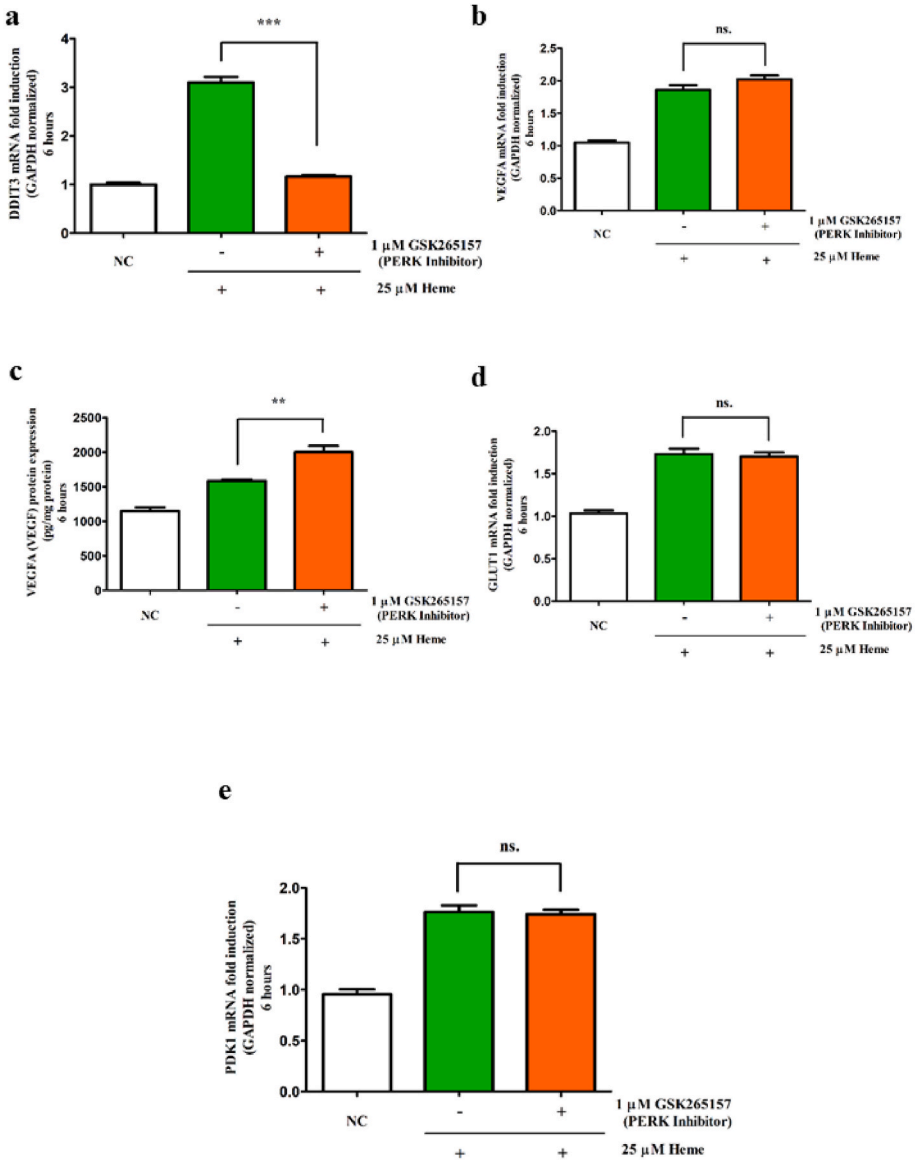

Fig. 9. ER stress are not connected to heme-induced VEGFA production in ARPE-19 cells. **a** CHOP gene expression in ARPE-19 cells exposed to heme (25 μM) and the PERK inhibitor GSK2656157 (1 μM). **b** VEGFA gene expression and **c** protein levels in ARPE-19 cells exposed to heme (25 μM) and the PERK inhibitor GSK2656157 (1 μM). NC: non-treated cells. **d** Gene expression levels of GLUT1 and **e** PDK1 in ARPE-19 cells exposed to heme (25 μM) and the PERK inhibitor GSK2656157(1 μM). NC: non-treated cells. Data are represented as mean value ± SEM (n = 6). Statistical analysis was performed by one-way ANOVA test followed by Bonferroni correction. A value of $p < 0.05$ was considered significant.

[61] and Krüppel-like factor 4 (KLF4) [62], were higher in heme-treated ARPE-19 cells. Given the relatively high expression of many genes involved in ROP/DR and genes of angiogenesis in ARPE-19 cells treated with heme, these data support our observation that hemorrhage possibly plays an important role in the pathology of ROP and DR.

HIF-1α is involved in the pathogenesis of both in the first and the second clinical phases of ROP [63], moreover in DR [64] by regulating VEGFA expression. Our study showed that heme facilitates nuclear translocation of HIF-1α in ARPE-19 cells. This is in good agreement with a study on experimental intracerebral hemorrhage, HIF-1α protein levels are significantly increased after intracerebral injection of lysed erythrocytes [65]. In addition, we showed that heme increased expression of hypoxia-regulated genes GLUT1 [31] and PDK1 [32], both involved in the pathology of DR and ROP [33,34].

The expression of VEGFA plays a crucial role in the pathogenesis of ROP [6], age-related macular degeneration (AMD) [66], and DR [28]. Here we observed that heme induces VEGFA expression and secretion in ARPE-19 cells. This is in close agreement with a previous study showing that heme upregulated VEGFA expression in rat vascular smooth muscle cells [38]. We also demonstrated that the heme-scavenger alpha-1-microglobulin (A1M) [67] efficiently blunted heme-induced VEGFA expression in ARPE-19 cells. These data suggest that retinal hemorrhage may further aggravates retinal neovascularization by inducing VEGFA expression.

To complement angiogenic signaling end points, we performed tube formation assay using ARPE-19 cell culture supernatants. Our results showed that HUVECs formed capillary-like structures in response to ARPE-19 cell culture supernatants that was markedly promoted by heme. This further supports our finding that heme can induce complex response in ARPE-19 cells that may aggravate angiogenesis and capillary formation.

Inhibiting HO-1 activity by SnPPIX downregulates both heme- and hypoxia-induced VEGFA production in vascular smooth muscle cells [38]. SnPPIX blocks the release of VEGFA from tumor cells [37].

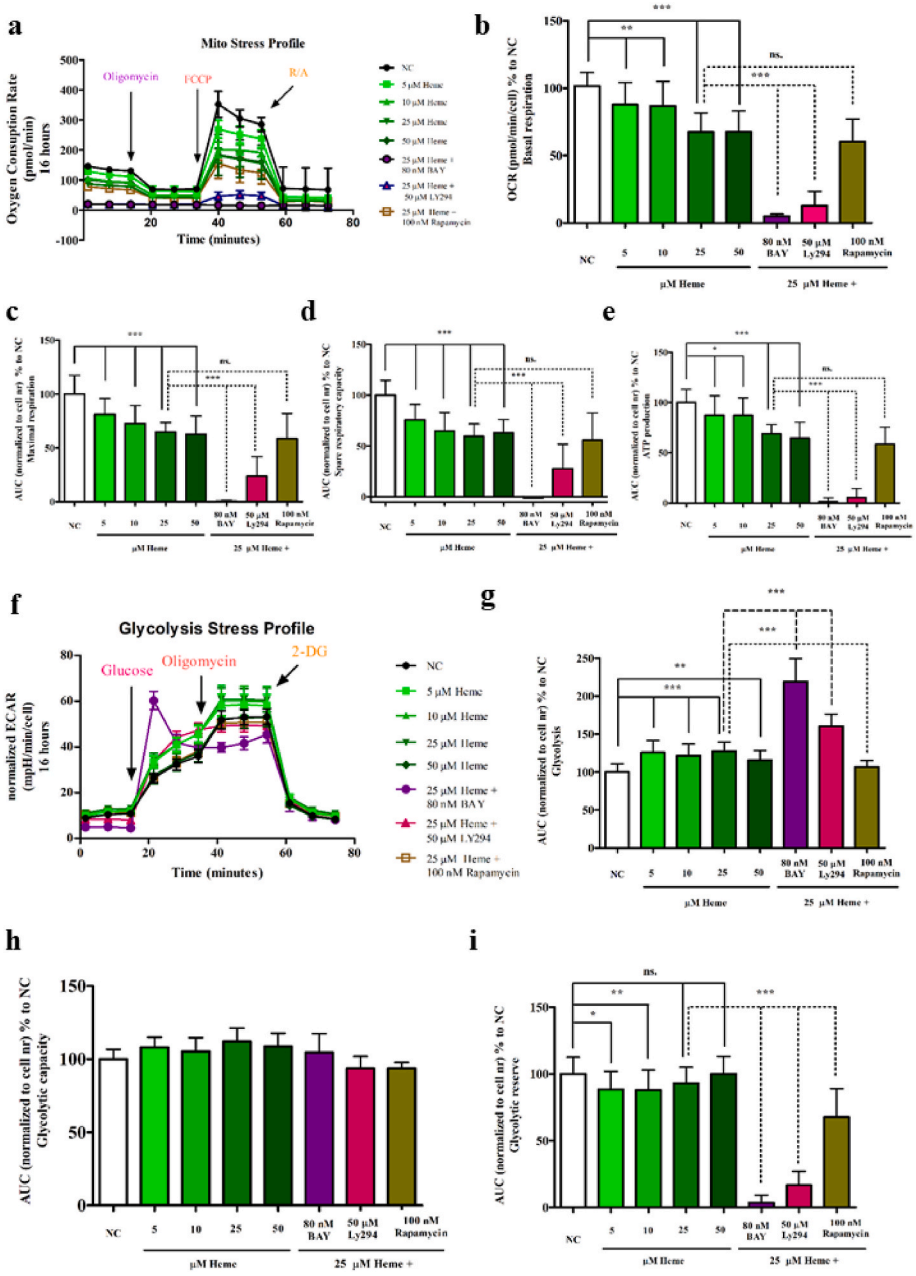

Fig. 10. Metabolic shift towards glycolysis in ARPE-19 cells exposed to heme. **a** Mito Stress Profile of ARPE-19 cells exposed to heme (5–50 μM) and heme (25 μM) + BAY 87–2243 (80 nM) or LY294002 (50 μM) or Rapamycin (100 nM). NC: non-treated cells. Data are represented as mean value ± SEM (n = 3). Statistical analysis was performed by one-way ANOVA test followed by Bonferroni correction. A value of $p < 0.05$ was considered significant. **b** Basal respiration, **c** maximal respiration, **d** spare respiratory capacity, and **e** ATP production of ARPE-19 cells exposed to heme (5–50 μM) and heme (25 μM) + BAY 87–2243 (80 nM) or LY294002 (50 μM) or Rapamycin (100 nM). NC: non-treated cells. Data are represented as mean value ± SEM (n = 3). Statistical analysis was performed by one-way ANOVA test followed by Bonferroni correction. A value of $p < 0.05$ was considered significant. **f** Glycolysis Stress Profile of ARPE-19 cells exposed to heme (5–50 μM) and heme (25 μM) + BAY 87–2243 (80 nM) or LY294002 (50 μM) or Rapamycin (100 nM). NC: non-treated cells. Data are represented as mean value ± SEM (n = 3). Statistical analysis was performed by one-way ANOVA test followed by Bonferroni correction. A value of $p < 0.05$ was considered significant. **g** Glycolysis, **h** glycolytic capacity, and **i** glycolytic reserve of ARPE-19 cells exposed to heme (5–50 μM) and heme (25 μM) + BAY 87–2243 (80 nM) or LY294002 (50 μM) or Rapamycin (100 nM). NC: non-treated cells. Data are represented as mean value ± SEM (n = 3). Statistical analysis was performed by one-way ANOVA test followed by Bonferroni correction. A value of $p < 0.05$ was considered significant.

Contrary to expectations, SnPPIX and HO-1 mRNA silencing had no effect on VEGFA expression in heme-treated ARPE-19 cells. Similarly, there was no effect of HO-1 inhibition on GLUT1 or PDK1 levels in heme-treated ARPE-19 cells. Our data suggest that retinal neovascularization in hemorrhagic retinopathies is likely to be HO-1 independent.

There is evidence that heme activates the TLR4 signaling [42]. TLR4 signaling participates in OIR, as TLR4 inhibitor TAK242 inhibits pathological neovascularization in DR model [41]. In order to test whether TLR4 is involved in the heme-induced expression of VEGFA, we exposed RPE cells to heme and inhibited the TLR4 signaling pathway with TAK242. Our data showed that heme-induced VEGFA expression in ARPE-19 cells is independent of TLR4 signaling.

Pathologic retinal angiogenesis in ROP and DR is associated with elevated levels of HIF-1α and VEGFA [68,69]. Inhibition of HIF-1α suppressed VEGFA expression and inhibited angiogenesis in a

a

Gene ID	Gene Symbol	Description	p (Corr)	Regulation	FC	Log FC
ENSG00000112096	SOD2	superoxide dismutase 2, mitochondrial	0.0156	down	-1.1780	-0.23628
ENSG00000134202	GSTM3	glutathione S-transferase mu 3	0.0142	up	1.0967	0.13321
ENSG00000008394	MGST1	microsomal glutathione S-transferase 1	0.0339	up	1.2164	0.28266
ENSG00000100983	GSS	glutathione synthetase	0.0272	down	-1.1417	-0.19121
ENSG00000104687	GSR	glutathione-disulfide reductase	0.0009	up	1.5184	0.60253
ENSG00000134202	GSTM3	glutathione S-transferase mu 3	0.0142	up	1.0967	0.13321
ENSG00000138780	GSTCD	glutathione S-transferase C-terminal domain containing	0.0042	down	-1.2252	-0.29301
ENSG00000143198	MGST3	microsomal glutathione S-transferase 3	0.0479	up	1.1204	0.16395
ENSG00000211445	GPX3	glutathione peroxidase 3	0.0032	up	1.2047	0.26871
ENSG00000100348	TXN2	thioredoxin 2	0.0364	down	-1.1077	-0.14760
ENSG00000136810	TXN	thioredoxin	0.0010	up	1.3571	0.44049
ENSG00000197763	TXNRD3	thioredoxin reductase 3	0.0225	down	-1.3047	-0.38371
ENSG00000198431	TXNRD1	thioredoxin reductase 1	0.0039	up	1.2780	0.35390
ENSG00000117450	PRDX1	peroxiredoxin 1	0.0047	up	1.1699	0.22633
ENSG00000117592	PRDX6	peroxiredoxin 6	0.0127	down	-1.1165	-0.15899
ENSG00000271303	SRXN1	sulfiredoxin 1	0.0015	up	1.5548	0.63676
ENSG00000100292	HMOX1	heme oxygenase 1	0.0001	up	14.4757	3.85556

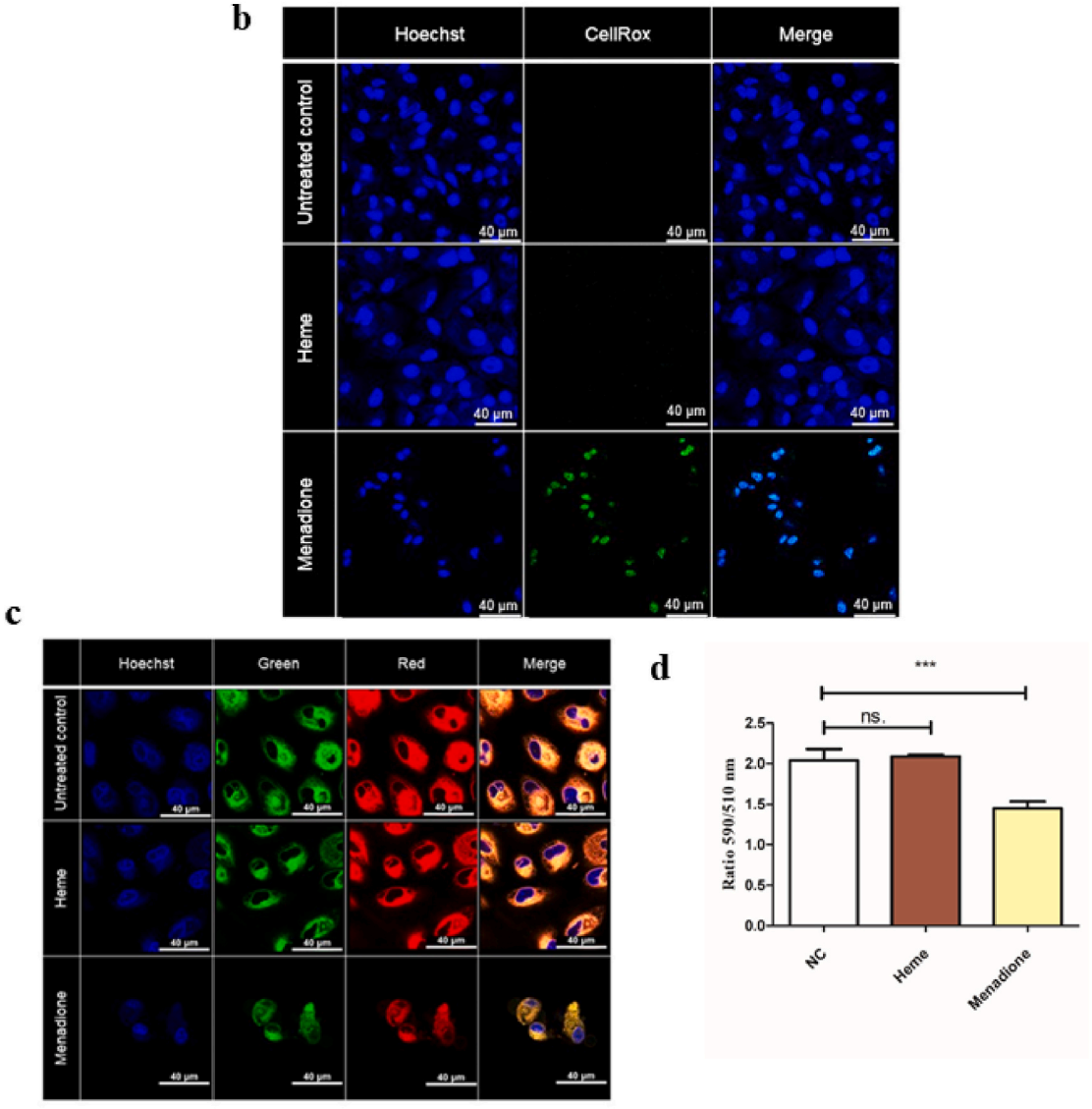

Fig. 11. Oxidative stress and antioxidant response of ARPE-19 cells in response to heme. **a** Significantly induced differently expressed genes (DEGs) identified in ARPE-19 cells exposed to heme (25 µM) compared to the control (n = 3). FC: fold induction, p (corr): corrugated p values. **b** Detection of reactive oxygen species in ARPE-19 cells using CellRox staining. Nuclei were visualized with Hoechst. **c** Detection of lipid peroxidation in ARPE-19 cells using BODIPY™ 581/591C11 reagent. Nuclei were visualized with Hoechst. **d** Ratio of 590/510 nm fluorescence intensities quantitated using LasX software. Ratios of the signal from red to green channels were used to quantify lipid peroxidation in cells (n = 3).

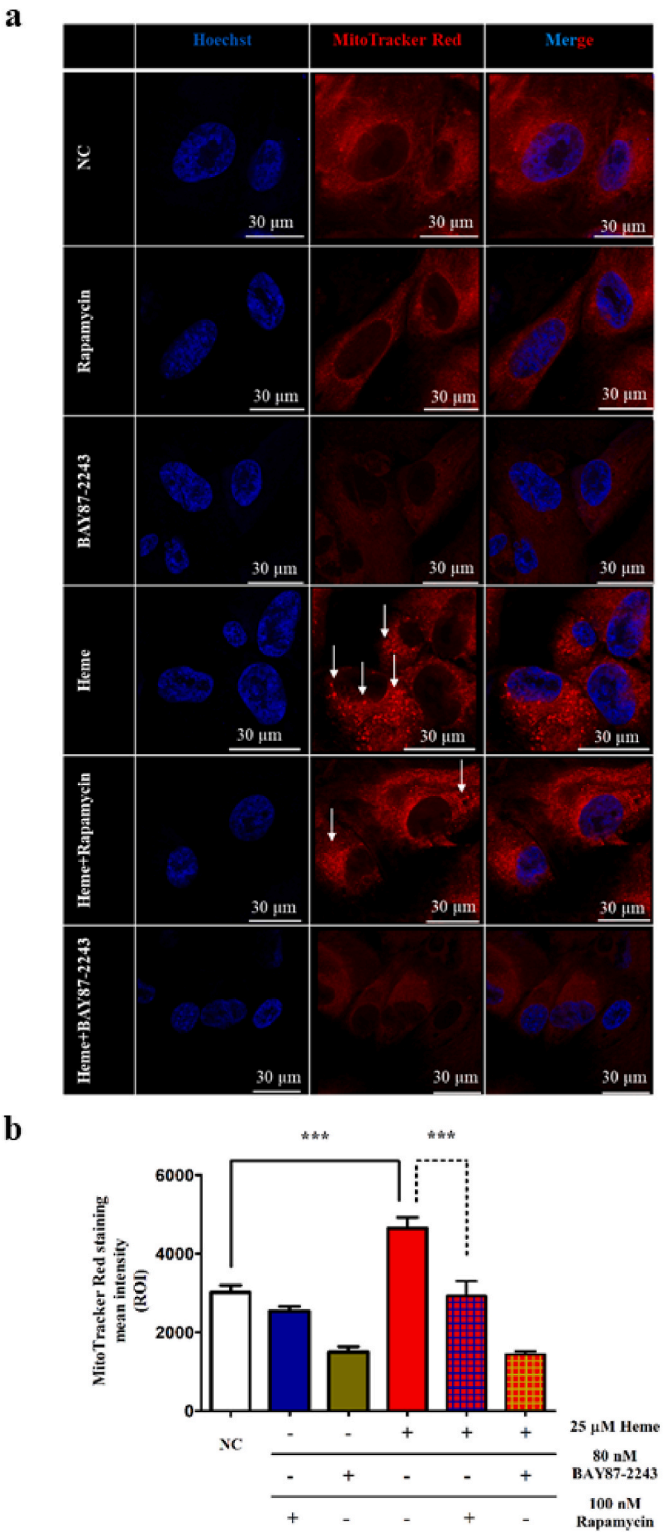

Fig. 12. Heme induces the aggregation of mitochondria in ARPE-19 cells. **a** ARPE-19 cells were exposed to heme (25 μM) alone or in combination with BAY 87–2243 (80 nM) or Rapamycin (100 nM) followed by Mitotracker Red staining (n = 3). Nuclei were visualized by Hoechst. White arrows indicate aggregated mitochondria. **b** Quantification of Region of interest (ROI). Ten individual ROIs (1 μm^2) were quantified and data are represented as mean value ± SEM. Statistical analysis was performed by one-way ANOVA test followed by Bonferroni correction. A value of $p < 0.05$ was considered significant.

time-dependent manner in animal model [64]. Since heme induces a hypoxic response through HIF-1α nuclear translocation and hypoxic gene expression in the ARPE-19 cells, we tested whether BAY 87–2243, a known inhibitor of HIF-1α, counteracts heme-induced VEGFA production and hypoxic response. We found that the heme-induced hypoxic response and VEGFA production were also counteracted by pharmacological inhibition of HIF-1α, which suggests that HIF-1α inhibitors can be used not only in hemorrhage-induced retinopathies.

Laser photocoagulation and anti-VEGFA agents are effective therapeutic practice in ROP [70] and DR [71]. However, severe adverse side effects of anti-VEGFA therapy have been reported [72]. These findings point to the need for new therapeutic approaches for the reduction of VEGFA expression without adverse side effects in ROP, AMD, and DR.

The PI3K/Akt/VEGFA signaling plays an important role in retinal angiogenesis [73]. Our results suggest that heme activates the PI3K/Akt pathway in the ARPE-19 cells, which may be involved in the heme-driven expression of VEGFA. PI3K inhibition by LY294002 inhibits retinal neovascularization in an OIR model [74]. We have shown here that LY294002 inhibits heme-induced VEGFA production, suggesting that LY294002 is likely to inhibit hemorrhage-induced neovascularization. LY294002 is also an inhibitor of the mTOR pathway [75]. Therefore, we cannot exclude the possibility that the protective effect of LY294002 on heme-driven VEGFA production may be due to its inhibitory potential on mTOR. Further work is needed to evaluate the anti-angiogenic potential of more selective PI3K inhibitors that have minimal toxicity.

To investigate the role of mTOR in heme-induced VEGFA expression, ARPE-19 cells were treated with rapamycin, a specific mTOR inhibitor. Rapamycin has anti-angiogenic effects by suppressing the HIF/VEGFA signaling pathway in the OIR [76] and in the DR model [77]. We have demonstrated that rapamycin is effective in the reduction of heme-induced VEGFA production and hypoxic response. Our results also support the possible therapeutic potential of rapamycin in the treatment of hemorrhagic retinopathies.

ER stress is involved in DR [78]. Inhibition of the PERK arm of the ER stress pathway reduces the expression of both CHOP and VEGFA in retinal pigment epithelial cells [50], whereas inhibition of the CHOP-HIF1α-VEGFA axis reduces retinal neovascularization in OIR [79]. We have shown earlier that heme activates ER stress in vascular endothelial cells [80]. Although heme induced CHOP expression in ARPE-19 cells, which was inhibited by PERK inhibitor, our results did not support activation of the PERK/CHOP/VEGFA axis in heme-treated ARPE-19 cells, suggesting that VEGFA production in ARPE-19 cells may occur independently of ER stress in response to bleeding.

Hypoxia and oxidative stress have been identified as significant factors in the development of AMD [81] and DR [82]. Hypoxia can lead to the generation of ROS, and heme itself is free radical catalyst that sensitizes cells towards oxidant-mediated killing and lipid peroxidation [83]. Based on these data we decided to test the cellular heme effect on the free radical metabolism. Here we showed that heme did not induce ROS generation and lipid peroxidation in ARPE-19 cells. Although heme significantly affected the expression of many genes involved in antioxidant response, these expressions showed heterogeneous pattern since certain antioxidant genes were significantly decreased (SOD2, GSS, GSTCD, TXN2, TXNRD3, PRDX6), while others genes significantly increased (GSTM3, MGST1, GSR, GPX3, TXN, TXNRD1, PRDX1). In addition to that, we did not detect cytotoxicity as a sign of oxidant-mediated cell death in ARPE-19 cells even at the high heme concentrations. These suggest that heme-driven hypoxic response and decreased oxidative phosphorylation in the mitochondria is presumably not associated with cell death and ROS generation or lipid peroxidation in ARPE-19 cells under our experimental condition.

Mitochondrial damage is involved in retinopathies [51,52]. We have shown that heme induces morphological changes in ARPE-19 cells. These changes may lead to a functional decline as indicated by decreased oxygen consumption. This was further exacerbated by BAY

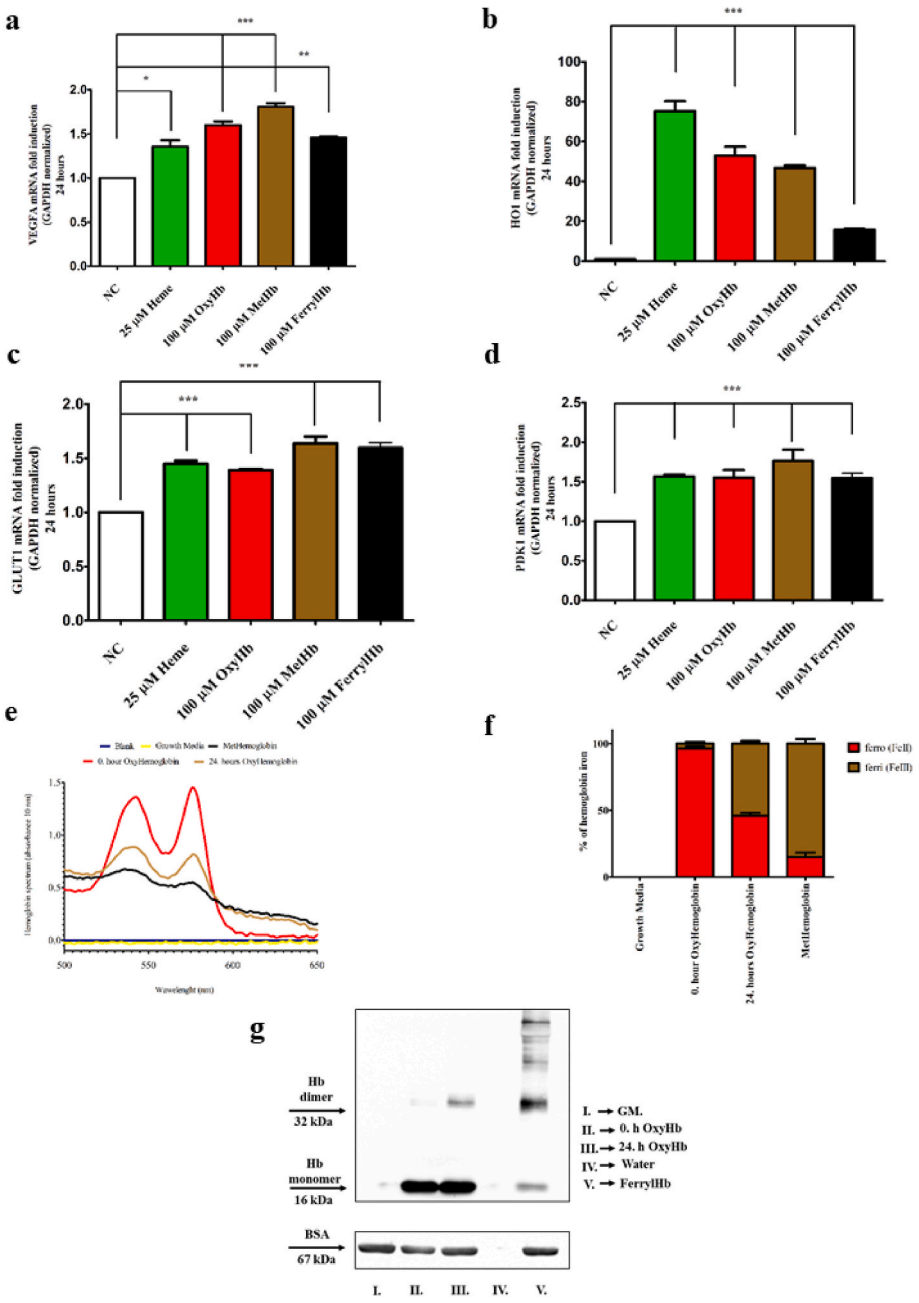

Fig. 13. Hemoglobins induce VEGF, PDK-1, and GLUT-1 expressions in ARPE-19 cells. **a** VEGFA, **b** HO-1, **c** GLUT-1, and **d** PDK-1 gene expression levels in ARPE-19 cells exposed to heme (25 μM), OxyHb (100 μM), MetHb (100 μM), and FerrylHb (100 μM) for 24 h. NC: non-treated cells, Hb: hemoglobin. **e** Oxidation process of OxyHb in ARPE-19 cell cultures measured by the oxidation states of the heme-iron by analyzing the absorbance spectra (500–650 nm) of Hbs. MetHb was used as a control of Hb oxidation. **f** Hb ratios were calculated as described previously by Winterbourn [95]. **g** Hb oxidation in cell culture supernatants was analyzed using immunoblotting by detecting of cross-linked Hb, using HRP-conjugated goat anti-human Hb polyclonal antibody. Bovine serum albumin (BSA) as a loading control was detected in cell culture supernatants with anti-BSA specific antibody NC: non-treated cells. Data are represented as mean value ± SEM (n = 3). Statistical analysis was performed by one-way ANOVA test followed by Bonferroni correction. A value of $p < 0.05$ was considered significant.

87–2243 and LY294002. This effect of BAY 87–2243 can be explained by the fact that BAY 87–2243 is a potent mitochondrial complex I inhibitor [84]. We detected an increase in glycolysis in response to heme. Energy metabolism of the RPE appears to play a fundamental role in photoreceptor function and death. Increased glycolysis leading to more robust glucose consumption in the RPE layer induces photoreceptor degeneration [85], suggesting the possible detrimental effect of heme-induced glycolytic response of the RPE to the photoreceptors. Evidence shows that there is a link between angiogenesis and mitochondria. A class of anti-angiogenic agents with antitumor activity targets the mitochondria to induce endothelial cell death to prevent their integration into new blood vessels [86]. However, data on the connection between mitochondrial function and VEGF derive mainly from endothelial cells. VEGF enhances the mitochondrial functions including mitochondrial oxidative respiration and intracellular ATP levels in endothelial cells [87,88]. In contrast to these, we found that mitochondrial function is decreased in heme-exposed ARPE-19 cells 16h after the heme exposure, despite the elevated VEGFA protein level in the supernatant. Importantly, it could be possible that VEGF released in response to heme might compensate the decrease in mitochondrial function. The potential and intriguing role of mitochondrial aggregation in VEGF production in response to heme should be investigate in future studies.

Free heme and Hb plays a pathologic role in various human pathologies with hemolysis and hemorrhage [89]. Evidence shows that hemolysis products, specifically Hb itself, have profound effects on angiogenesis. Hb induces VEGF secretion in tumor cells [53]. Similar to this early report, we found that Hbs are capable of inducing VEGFA expression in ARPE-19 cells regardless its oxidation status supporting the notion that Hb itself is a potent angiogenesis inducer in the retina supporting the potential etiological role of hemolysis in retinal neovascularization. In addition, we found that Hbs, similar to heme, induce GLUT1 and PDK1 expression in ARPE-19 cells. It is important to note that upon oxidation, free Hb releases its heme moieties [19–22]. We found that Hb is being readily oxidized in ARPE-19 cell culture supernatants which raises the question whether the very Hb or its free heme moieity is responsible for its angiogenic potential. Therefore, further research is needed to explore whether Hb itself or its heme released upon Hb oxidation is responsible for VEGFA induction in ARPE-19 cells.

The main sources of retinal VEGFA are astrocytes in the ganglion cell layer, Müller cells in the inner nuclear layer, and the RPE [11]. Given that our study focuses on the RPE, it would be beneficial for future studies to investigate the potential impact of heme on VEGFA secretion from astrocytes and Müller cells. Another limitation of our work that RPE cells are mainly involved in choroidal neovascularization [90–92], which makes these cells an ideal model of choroidal neovascularization. However, RPE cells produce high levels of proangiogenic factors and maintain retinal and choroidal homeostasis [90–92]. The inner retina is often considered the primary region affected ROP, but choroidal involution and outer retinal dysfunctions also occur in ROP suggesting that ROP should no longer be considered an inner retinal vasculopathy only, but also a disease of choroidal degeneration affecting both RPE and photoreceptor integrity [93], which does not exclude that any hemorrhage reaching the RPE layer might have a role in ROP development.

Although we analyzed the association between hemorrhage and ROP severity in preterm patients, similar mechanistic implications in ROP, DR, and AMD raise the hypothesis that hemorrhage/heme may be involved in the etiology of DR and AMD. Heme, as an amphipathic an easily diffusible agent, may reach any cells in the retinal tissue after bleeding, among them ARPE-19 cells, and induces high levels of proangiogenic factors.

The presented data help us to understand the pathological role of retinal hemorrhage in ROP and DR. Our results highlight the substantial involvement of HIF-1α-driven hypoxic response and activation of pathways involved in angiogenesis as well as mitochondrial damage in response to heme in the ARPE-19 cells. This study provides evidence that inhibitors of HIF-1α and PI3K as well as the mTOR inhibitor rapamycin may have therapeutic potential in retinopathies associated with hemorrhage.

4. Methods

4.1. Ethics approval

Retrospective analysis of clinical data was approved by the Regional Research Ethical Committee of University of Debrecen under Project No.: DE RKEB/IKEB 5419-2020. and was conducted in accordance with the ethical standards of all relevant national and institutional committees and the World Medical Association's Declaration of Helsinki. The clinical part of the research was a retrospective study, so the Scientific and Research Ethics Committee of the University of Debrecen waived the need for informed consent from all subjects and/or their legal guardian(s).

4.2. Human premature newborn cohort selection

Our study to reveal the probable causative relationship between retinal hemorrhage and ROP started with retrospective clinical data analysis (Regional Research Ethical Committee Project No.: DE RKEB/IKEB 5419-2020). Since our tertiary neonatal intensive care unit (NICU-III) is part of the Vermont Oxford Network (VON), we were able to compare the incidence of stage 3 ROP and the rate of ROP treatment in this population on international level. Our focus was the population of inborn premature newborns under 29 weeks of gestational age during the last ten-year period. The VON database contained 370000 screened cases for ROP according to these characteristics. Both the rate of stage 3 ROP and the rate of ROP treatment were collected from the database and were given in percentage of the screened newborns broken down by year.

In the second set of our clinical study, we formed two groups of premature newborns in our NICU-III having stage 3 ROP without or with retinal hemorrhage at any time of ROP screening process. As our clinic is the center of eastern region of Hungary for ROP laser treatment, ophthalmic- and brain surgery, we were able to collect 824 cases with stage 3 ROP at gestational weight under 1500 g during the years of 2008–2020. From these premature newborns, 145 patients formed the so called hemorrhaged ROP patients, who presented stage 3 ROP together with retinal hemorrhage. The randomized selection of the non-hemorrhaged group was based on the medical history of the first 145 patients without hemorrhage status according to the weight and gestational week. Importantly, the two groups did not differ in gestational age and birth weight. In order to prove the probable pathophysiological effect of retinal hemorrhage in ROP progression, we used the rate of ROP treatments as indicators for ROP aggravation in the established groups.

Moreover, from the 145 hemorrhaged ROP patients we could find 40 cases, where only one eye suffered retinal bleeding; in this way, 80 eyes were subjected to additional analysis. In order to prove the possible pathophysiological effect of retinal hemorrhage in the mechanism of ROP in the one eye bleeding cohort, the activity of neovascularization was selected to be the outcome measure.

4.3. ROP screening, treatment, activity of neovascularization

Screening was performed by an experienced ophthalmologist in ROP using Ret-Cam, occasionally binocular ophthalmoscopy, according to the current guidelines [94,95]. Any type of hemorrhage during the screening period was considered to be retinal bleeding. Indications of ROP treatment were carried out according to the recommendation of the Early Treatment for ROP Collaborative Group (ET-ROP) [95,96]. To measure the activity of the neovascularization, the latest ICROP recommendation was followed. The vascular abnormality is a spectrum, based on the engorgement and tortuosity of the retinal vessels starting from the normal to plus disease. Normal vessels with zero value do not represent pathology, while preplus disease is marked by one point, and plus disease gets 2. These values were multiplied by the extent of vascular pathology based on the "clock hours", and the summary value was given for one eye [95].

4.4. Reagents

Reagents were purchased from Sigma-Aldrich (St. Louis, MO, US) unless otherwise specified. Hemin chloride stock solution was prepared protected from light in sterile 20 mM NaOH on the day of use for each experiment. BAY 87–2243, LY294002, and Rapamycin were purchased from MedChemExpress (Bergkällavägen, Sollentuna, Sweden). Tin-protoporphyrin IX (SnPPIX) was purchased from Santa Cruz Biotechnology (Dallas, TX, US) or Cayman Chemical (Ann Arbor, MI, US). TAK-242 was obtained from Cayman Chemical.

4.5. Cell culture

Human retinal pigment epithelial cells (ARPE-19 cells; Cat. No. CRL-2302) was obtained from ATCC (Manassas, VA, US). Cells were grown in Dulbecco's Modified Eagle Medium (DMEM): F-12 Medium (ATCC, Manassas, VA, US)) with 10 % FBS, 100 U/mL penicillin, 100 μg/mL

streptomycin, and amphotericin B until passages 4. From passage 4, cells were maintained in low glucose DMEM (Biosera, Cholet, France) supplemented with 15 mM HEPES pH 7.3, 10 % fetal bovine serum (Thermo Fisher Scientific, Waltham, MA, US), 100 U/mL penicillin, 100 μg/mL streptomycin, and amphotericin B (culture medium, CM). The medium was changed every 2 days. Cells between passage 5 and 8 were used for the experiments. Heme treatments were carried out in serum- and antibiotic-free CM. Briefly, hemin chloride stock solution in sterile 20 mM NaOH was diluted in serum- and antibiotic-free CM. Cells were washed twice with Phosphate Buffered Saline (PBS) pH 7.4 (Biosera, Cholet, France) and treated with heme for 1 h in CM without serum and antibiotics. Cells were then washed with PBS and fresh CM with 10 % fetal bovine serum (FBS) and antibiotics were added and cells were further incubated for 6 h, and 16 h in a CO_2 (5 %) incubator. In some experiments, cells were pre-treated either with SnPPIX (25 μM), or LY294002 (50 μM), or Rapamycin (100 nM), or BAY 87–2243 (20–80 nM), or GSK2656157 (1 μM) for 1 h in CM, then exposed to heme as described above in the presence of either SnPPIX (25 μM), or LY294002 (50 μM), or Rapamycin (100 nM), or BAY 87–2243 (20–80 nM), or GSK2656157 (1 μM), washed, then further incubated in CM in the presence of either SnPPIX (25 μM), or LY294002 (50 μM), or Rapamycin (100 nM), or BAY 87–2243 (20–80 nM), or TAK-242 (3 μM), or GSK2656157 (1 μ) for 6 or 16 h.

To analyze the effect of Hbs of different redox states, ARPE-19 cells were expose to heme (25 μM), OxyHb (100 μM), MetHb (100 μM), and FerrylHb (100 μM) in growth medium supplemented with 2.5 % of FBS for 24 h. In some experiments, alpha-1-microglobulin (A1M) was added to heme (25 μM) diluted in serum- and antibiotic-free DMEM to a concentration of 12.5 μM of rA1M, gently mixed then incubated at room-temperature in the dark with gentle agitation for 30 min. Then, heme-rA1M complexes were added to the cells as described above.

4.6. Proteome Profiler Human Angiogenesis Array

Proteome Profiler Human Angiogenesis Array (R&D Systems, Abingdon, UK) was performed according to the manufacturer's guide. Briefly, cells were exposed to heme as described above and supernatants were collected after 16h. Each group contained two replicates of culture supernatant mixtures. Membranes were imaged with iBright FL1500 (Thermo Fisher Scientific, Waltham, MA, US).

4.7. RNA isolation and quantitative reverse transcription-polymerase chain reaction

Cells were treated as described earlier by heme and the different inhibitors. RNA isolations were performed 6 h after the heme treatments. Cells were grown on six-well plates and total RNA was isolated with TriReagent (Zymo Research, Irvine, CA, US) and reverse-transcribed using High-Capacity cDNA Reverse Transcription Kit (Applied Biosystems Inc., Foster City, CA, US). VEGFA (Hs00900055_m1), HO1 (Hs01110250_m1) GLUT1 (Hs00892681_m1), PDK1 (Hs01561847_m1), DDIT3 (Hs00358796_g1), ANG (Hs04195574_sh) and GAPDH (Hs02786624_g1) mRNA expressions were determined by TaqMan Gene Expression Assays (Thermo Fisher Scientific, Waltham, MA, US). Expressions were normalized to GAPDH. Reverse transcriptions and qPCRs were carried out using the C1000 Thermal Cycler with CFX 96 Real-Time PCR System (Bio-Rad, Hercules, CA, US). Relative mRNA expressions were calculated with the ΔΔCt method using GAPDH as an internal control.

4.8. Cell lysis and immunoblot

Cells were treated as described earlier by heme. Protein isolations were performed right after the heme treatments. Cells were washed with cold phosphate-buffered saline pH 7.4 then lysed with RIPA buffer containing protease and phosphatase inhibitors (50 mM Tris pH 7.5, 150 mM NaCl, 1 % Igepal CA-630, 1 % Sodium-deoxycholate, 0.1 % SDS, 1 × Complete Mini Protease Inhibitor Cocktail, 1 × PHOSSTOP phosphatase inhibitor cocktail, and incubated for 15 min on ice. Lysates were clarified by spinning at 16,000×*g*, 4 °C for 15 min. Protein content was determined using the bicinchoninic acid assay (Pierce BCA Protein Assay Kit, Thermo Fisher Scientific, Waltham, MA, US). Cell extracts were electrophoresed on Tris–glycine SDS-PAGE gels, then the proteins were transferred to 0.45 μm nitrocellulose membrane (GE Healthcare, Chicago, IL, US) and blocked with 5 % w/v milk (Bio-Rad, Hercules, CA, US) for 60 min according to the manufacturer's guide. Primary antibodies against Akt (pan) (Cat. No. 4691) and Phospho-Akt (Ser473) (Cat. No. 4060) from Cell Signaling Technology (Danvers, MA, US) were diluted 1:2000 and incubated at 4 °C overnight, washed three times, then incubated with Anti-rabbit IgG, HRP-linked Antibody (Cell Signaling Technology, Danvers, MA, US) Protein loading was normalized to total protein content using No-Stain™ Protein Labeling Reagent (Thermo Fisher Scientific, Waltham, MA, US). The antigen–antibody complex was detected by WesternBright Quantum HRP substrate (Advansta, Menlo Park, CA, US). Immunoblots were imaged with iBright FL1500 (Thermo Fisher Scientific, Waltham, MA, US). Equal protein loading was followed by No-Stain™ Protein Labeling Reagent (Thermo Fisher Scientific, Waltham, MA, US).

4.9. siRNA transfection

Silencer select small interfering RNA specific to HO1 and non-targeting siRNA were obtained from Ambion (Thermo Fisher Scientific, Waltham, Massachusetts, US). RPE transfection with siRNA was achieved using the Oligofectamine (Thermo Fisher Scientific, Waltham, MA, US) according to the manufacturer's guide in OPTI-MEM Reduced Serum Medium (Thermo Fisher Scientific, Waltham, MA, US). Transfection mixtures were let on the cells for 24 h. Cells were then treated with heme and the different inhibitors as described above. RNA isolations were performed 6 h after the heme treatments.

4.10. Human VEGFA quantikine ELISA

Supernatants from RPEs exposed to heme and inhibitors were collected and analyzed using Human VEGFA Quantikine ELISA assay (R&D Systems, Abingdon, UK) according to the manufacturer's guide. VEGFA expressions were normalized to protein content determined using the bicinchoninic acid assay (Pierce BCA Protein Assay Kit, Thermo Fisher Scientific, Waltham, MA, US). Supernatants were collected 16 h after the heme treatments.

4.11. RNA-seq method

RNA isolations were performed as described earlier. To obtain global transcriptome data high throughput mRNA sequencing analysis was performed on Illumina sequencing platform. Total RNA sample quality was checked on Agilent BioAnalyzer using Eukaryotic Total RNA Nano Kit (Agilent Technologies, Santa Clara, CA, US) according to manufacturer's protocol. Samples with RNA integrity number (RIN) value > 7 were accepted for library preparation process. RNA-Seq libraries were prepared from total RNA using Ultra II RNA Sample Prep kit (New England BioLabs, Ipswich, MA, US) according to the manufacturer's protocol. Briefly, poly-A RNAs were captured by oligo-dT conjugated magnetic beads then the mRNAs were eluted and fragmented at 94-Celsius degree. First strand cDNA was generated by random priming reverse transcription and after second strand synthesis step double stranded cDNA was generated. After repairing ends, A-tailing and adapter ligation steps adapter ligated fragments were amplified in enrichment PCR and finally sequencing libraries were generated. Sequencing run were executed on Illumina NextSeq 500 instrument (Illumina, San Diego, CA, US) using single-end 75 cycles sequencing.

4.12. RNA-seq data analysis

Raw sequencing data (fastq) was aligned to human reference genome version GRCh38 using HISAT2 algorithm and BAM files were generated. Downstream analysis was performed using StrandNGS software (www.strand-ngs.com). BAM files were imported into the software DESeq algorithm was used for normalization. Moderated T-test with Benjamini-Hochberg FDR correction was used to determine differentially expressed genes between conditions, p value < 0.05 was considered significant difference. Aligned sequencing data have been deposited into the NCBI SRA database under accession BioProject ID PRJNA1063912. https://dataview.ncbi.nlm.nih.gov/object/PRJNA1063912?reviewer=uchl3j5c1v0ktbopa94auahc06

4.13. Pathway analyses

CytoScape v3.4 software with ClueGo v2.3.5. application was used for identifying over-represented Gene ontology (GO) terms. Two-sided hypergeometric test was performed; the list of differentially expressed genes was tested against GO Biological process databases.

4.14. Confocal microscopy

Cells were grown on coverslips and treated with heme and inhibitors as described above. Phospho-Akt (Ser473) staining was performed right after the heme treatment. HIF-1α expression was analyzed 16 h after the heme treatment. For confocal analyses, cells were washed with PBS pH 7.4 twice and fixed with 4 % paraformaldehyde solution in PBS for 15 min at 37 °C. Coverslips were then washed three times with PBS pH 7.4, then blocked in Blocking Buffer (5 % normal goat serum/0.3 % Triton X-100 in PBS) for 60 min. Primary antibody against HIF-1α (dilution 1:400) (Cell Signaling Technology, Danvers, MA, US) and Phospho-Akt (Ser473) (dilution 1:400; Cell Signaling Technology, Danvers, MA, US) were diluted in antibody dilution buffer (1 % BSA/0.3 % Triton X-100 in PBS) and incubated overnight at 4 °C. Samples were then incubated then with goat anti-rabbit IgG conjugated to Alexa Fluor 488 (Thermo Fisher Scientific, Waltham, MA, US) (Thermo Fisher Scientific, Waltham, MA, US) at a dilution of 1:500 for 60 min. Nuclei were visualized with Hoechst. Samples were investigated with Lightning super-resolution microscopy using Leica Application Software X (Leica, Mannheim, Germany).

4.15. Hb preparations

Hbs of different redox states, that is, OxyHb, MetHb, and FerrylHb were prepared as described previously [97]. Briefly, Hb was purified from fresh blood drawn from healthy volunteers with ion-exchange chromatography on a DEAE Sepharose CL-6B column. To generate FerrylHb, purified Hb was incubated for 1 h at 37 °C with a 10:1 ratio of H_2O_2 to heme followed by dialysis against saline (3 times for 3 h at 4 °C) and concentration using Amicon Ultra centrifugal filter tubes (10,000 MWCO, Millipore Corp., Billerica, MA, USA). Aliquots were snap-frozen in liquid nitrogen and stored at −80 °C. The purity of each Hb preparation was measured by SDS-PAGE followed by staining with the ProteoSilver Plus Silver Staining Kit. The purity of Hb preparations was above 99.9 %. Hb concentrations were calculated as described by Winterbourn [98].

4.16. Measurement of Hb oxidation in ARPE-19 supernatants

To measure cell-driven oxidation of Hb in the ARPE-19 cell culture supernatants, cells were exposed to OxyHb (100 μM) for 24 h in growth medium supplemented with 2.5 % FBS. The oxidation process of Hb was followed by measuring the oxidation states of the heme-iron by analyzing the absorbance spectra (500–650 nm) of Hbs. MetHb was used as a control of Hb oxidation. Hb ratios were calculated as described previously by Winterbourn [98].

4.17. Detection of cross-linked hemoglobin by Western Blot

Hb oxidation was analyzed by immunoblotting, using HRP-conjugated goat anti-human Hb polyclonal antibody (Abcam, Cambridge, UK) as described earlier [99].

4.18. Cell viability assay

Cell viability was determined by the MTT assay. Briefly, cells were cultured and treated in 96-well plates for the indicated time with heme (10–300 μM). Then cells were washed with PBS, and 100 μL of 3-[4,5-dimethylthiazol-2-yl]-2,5-diphenyl-tetrazolium bromide (0.5 mg/mL) solution in Hank's Balanced Salt Solution with calcium and magnesium was added. After a 90-min incubation, the MTT solution was removed, formazan crystals were dissolved in 100 μL of DMSO and optical density was measured at 570 nm.

4.19. Detection of lipid peroxidation

Lipid peroxidation was measured with Image-iT Lipid Peroxidation Kit (Thermo Fisher Scientific, Waltham, MA, US) which uses the BODIPY™ 581/591C11 reagent to measure lipid peroxidation. To measure lipid peroxidation, ARPE-19 cells cultured in DMEM without phenol red as described above. Then, cells were plated to coverglass bottom culture dishes and exposed to heme (25 μM) for 1 h in CM without serum and antibiotics. Cells were then washed with PBS and fresh DMEM without phenol red supplemented with 10 % fetal bovine serum (FBS) and antibiotics, and cells were further incubated for 3 h in a CO_2 (5 %) incubator. Cells exposed to menadione (100 μM for 2 h) were used as lipid peroxidation control. Cells were stained with Hoechst 33342 and 10 μM of Lipid Peroxidation Sensor (Thermo Fisher Scientific, Waltham, MA, US) for 30 min incubated at 37 °C. Cells were then washed three times with phosphate buffered saline and imaged in Hank's Balanced Salt Solution with calcium and magnesium with Leica confocal microscope using filters for Hoechst, FITC and Texas Red channels. The signal was then quantitated using LasX software (Leica, Mannheim, Germany) and the ratios of the signal from red to green channels were used to quantify lipid peroxidation in cells.

4.20. Endothelial Cell Tube Formation Assay

The formation of endothelial cell tube networks was analyzed using Angiogenesis Starter Kit (GIBCO, Thermo Fisher Scientific). To produce conditioned culture media, ARPE-19 cells were exposed to heme (25 μM) as described above, washed, and cultured in Medium 200 supplemented with 2 % FCS for 16 h. Then, supernatants were concentrated 10-fold and 25-fold using Amicon Ultra Centrifugal Filter, 10 kDa MWCO (Merck, Darmstadt, Germany) according to the manufacturer's guide. Endothelial tube formation assay (In Vitro Angiogenesis) was performed as recommended by the Angiogenesis Starter Kit. Human Umbilical Vein Endothelial Cells (HUVECs) were cultured in Medium 200 supplemented with Large VesseI Endothelial Supplement (LVES). 35 mm Glass Bottom Dish (Ibidi, Gräfelfing, Germany) were coated with Geltrex LDEV-Free Reduced Growth Factor Basement Membrane Matrix according to the manufacturer's guide. HUVECs were trypsinized and resuspended in Medium 200 containing 2 % FBS without LVES. Then, 75,000 cells (in a maximal final volume of 110 μl) in Medium supplemented with 2 % FBS without LVES were plated in 1 ml of tenfold- or twentyfive-fold concentrated conditioned supernatants from ARPE-19 cells and incubated for 16 h. As a positive control of tube formation, HUVECs were plated in Medium 200 supplemented with LVES. HUVECs plated in Medium 200 with 2 % FBS without LVES served as negative controls. Tube formation was observed using Leica DMi1 microscope.

4.21. Cellular energetics

The oxygen consumption rate (OCR), and extracellular acidification rate (ECAR) were measured by Seahorse XFe96 Extracellular Flux analyzer (Agilent Technologies, Santa Clara, CA, US). ARPE-19 cells were cultured overnight in 96 well Seahorse plates at a density of 2×10^4 cells/well, in DMEM growth. Cells were exposed to heme and the different inhibitors as described above. After 16h, assays were run in XF Assay Medium supplied with 1 g/L glucose, 1 mM sodium pyruvate and 2 mM L-glutamine for Mitochondrial Stress Test, or 2 mM L-glutamine for Glycolysis Stress Test according to manufacturer's instruction. For Mitochondrial Stress Test, compounds were injected at final concentrations of: 1.5 μM oligomycin, 0.5 μM carbonyl cyanide-4-(trifluoromethoxy) phenylhydrazone (FCCP), and 0.5 μM rotenone/antimycinA. For a Glycolysis Stress Test, we used final concentrations of 10 mM glucose, 1.5 μM oligomycin, and 50 mM 2-Deoxy-D-glucose (2-DG). OCR and ECAR values were normalized to cell number carried out by Sulforhodamine B (SRB) staining. Briefly, cells were fixed with 10 % TCA followed by SRB stain. Excess of stain were washed out by 1 % acetic acid. Finally, precipitate was reconstituted by Tris buffered saline and absorbance was measured at 570 nm (BioTek, Epoch2 plate reader, Agilent Technologies, Santa Clara, CA, US). Parameters were calculated by Wave 2.6.3 Software (Agilent Technologies, Santa Clara, CA, US) and expressed in percentage to NC. Experiments were repeated three times on different days.

4.22. Lactate measurement

Lactate measurements in cell culture supernatants were performed by Radiometer ABL90 (Radiometer UK Limited, Crawley, UK) 16 h after the heme treatment.

4.23. Mitotracker Red Staining

RPEs were grown on coverslips and treated with heme and inhibitors as described above. Mitotracker Red Staining were performed 16 h after the heme treatments. Cells were then incubated with 0.25 μM of Mitotracker Red (Thermo Fisher Scientific, Waltham, MA, US) in CM for 30 min at 37 °C/5 % CO_2, rinsed with CM and fixed with 4 % paraformaldehyde solution in CM for 15 min at 37 °C followed by three washes with PBS. Nuclei were visualized with Hoechst. Samples were investigated with Lightning super-resolution microscopy using Leica Application Software X (Leica, Mannheim, Germany). Ten individual Region of interest (ROIs) (1 μm^2) were quantified by using Leica Application Software X (Leica, Mannheim, Germany) and data are represented as mean value ± SEM.

4.24. Detection of oxidative stress

ARPE-19 cells were exposed to heme (25 μM) for 1 h in CM without serum and antibiotics. Cells were then washed with PBS and fresh CM with 10 % fetal bovine serum (FBS) and antibiotics were added and cells were further incubated for 3 h in a CO_2 (5 %) incubator. Cells exposed to menadione (200 μM for 1 h) were used as oxidative stress control The cells were then stained with 5 μM CellROX Green Reagent (Thermo Fisher Scientific, Waltham, MA, US) by adding the probe to the complete media and incubating at 37 °C for 30 min. Cells were then washed three times with phosphate buffered saline, fixed with 3.7 % paraformaldehyde solution. Nuclei were stained with Hoechst and samples were immediately analyzed using confocal microscopy (Leica, Mannheim, Germany).

4.25. Statistical analysis

Statistical analysis was performed by one-way ANOVA test followed by Bonferroni correction. A value of $p < 0.05$ was considered statistically significant. GraphPad Prism 5.0 software (GraphPad Software, Boston, MA, US) was used for statistical evaluation of the data. Data are represented as mean value ± SEM. Moderated T-test was used to determine differentially expressed genes between conditions, $p < 0.05$ was considered significant difference.

Data availability

The data that support the findings of this study are available upon request from the corresponding author G.B.

CRediT authorship contribution statement

Tamás Gáll: Conceptualization, Investigation, Writing – original draft, Writing – review & editing. **Dávid Pethő:** Investigation, Methodology. **Katalin Erdélyi:** Investigation, Methodology. **Virág Egri:** Methodology. **Józon György Balla:** Investigation. **Annamária Nagy:** Investigation. **Annamária Nagy:** Investigation, Methodology. **Szilárd Póliska:** Investigation, Methodology. **Magnus Gram:** Methodology. **Róbert Gábriel:** Methodology. **Péter Nagy:** Methodology. **József Balla:** Funding acquisition, Supervision, Writing – original draft, Writing – review & editing. **György Balla:** Supervision.

Declaration of competing interest

The authors have declared no conflict of interest.

Acknowledgements

The research group is supported by Hungarian Research Network (11003). This work was supported by Hungarian Government grants, OTKA-K 132828 (J.B.). The project was co-financed by the European Union and the European Social Fund: EFOP-3.6.2-16-2017-00006 (LIVE LONGER). Project no. TKP2020-NKA-04 has been implemented with the support provided by the Ministry of Innovation and Technology of Hungary from the National Research, Development and Innovation Fund, financed under the 2020-4.1.1-TKP2020 funding scheme. Project no. TKP2021-EGA-18 has been implemented with the support provided by the Ministry of Innovation and Technology of Hungary from the National Research, Development and Innovation Fund, financed under the TKP2021-EGA funding scheme. P.N. acknowledges the support from the National Research, Development and Innovation Fund of the Ministry of Culture and Innovation under the National Laboratories Program (National Tumor Biology Laboratory (2022-2.1.1-NL-2022-00010)) and the Hungarian Thematic Excellence Program (under project TKP2021-EGA-44) Grant Agreements with the National Research, Development and Innovation Office (NRDIO) and the HUN-REN – ATE – Laboratory of Redox Biology (grant 15002). The work was carried out at University of Debrecen, Kálmán Laki Doctoral School of Biomedical and Clinical Sciences. The Graphical abstract was created with BioRender.com.

Appendix A. Supplementary data

Supplementary data to this article can be found online at https://doi.org/10.1016/j.redox.2024.103316.

References

[1] W.S. Wright, R.S. Eshaq, M. Lee, G. Kaur, N.R. Harris, Retinal physiology and circulation: effect of diabetes, Compr. Physiol. 10 (2020) 933–974, https://doi.org/10.1002/cphy.c190021.
[2] C. Singh, Metabolism and vascular retinopathies: current perspectives and future directions, Diagnostics 12 (2022), https://doi.org/10.3390/diagnostics12040903.
[3] J. Woods, S. Biswas, Retinopathy of prematurity: from oxygen management to molecular manipulation, Mol Cell Pediatr 10 (2023) 12, https://doi.org/10.1186/s40348-023-00163-5.
[4] Q. Li, T. Han, Z. Wang, H. Tang, Z. Feng, Clinical characteristics, risk factors and short-term prognosis of retinopathy of prematurity complicated with retinal

hemorrhage, Eur. J. Ophthalmol. (2022) 11206721221136314, https://doi.org/10.1177/11206721221136314.
[5] T.L. Terry, Fibroblastic overgrowth of persistent tunica vasculosa lentis in infants born prematurely: II. Report of cases-clinical aspects, Trans. Am. Ophthalmol. Soc. 40 (1942) 262–284.
[6] J. Chen, L.E. Smith, Retinopathy of prematurity, Angiogenesis 10 (2007) 133–140, https://doi.org/10.1007/s10456-007-9066-0.
[7] H.W. Lim, S. Pershing, D.M. Moshfeghi, H. Heo, M.E. Haque, S.R. Lambert, Causes of childhood blindness in the United States using the IRIS® Registry (intelligent research in Sight), Ophthalmology (2023), https://doi.org/10.1016/j.ophtha.2023.04.004.
[8] E. Lo-Cao, S. Crofts, K. Geering, R.V. Jamieson, J.R. Grigg, Spectrum of ocular disease in children aged between 0 and 3 years at an Australian paediatric tertiary hospital, Clin. Exp. Ophthalmol. (2023), https://doi.org/10.1111/ceo.14237.
[9] R. Cayabyab, R. Ramanathan, Retinopathy of prematurity: therapeutic strategies based on pathophysiology, Neonatology 109 (2016) 369–376, https://doi.org/10.1159/000444901.
[10] A. Hellstrom, C. Perruzzi, M. Ju, E. Engstrom, A.L. Hard, J.L. Liu, K. Albertsson-Wikland, B. Carlsson, A. Niklasson, L. Sjodell, et al., Low IGF-I suppresses VEGF-survival signaling in retinal endothelial cells: direct correlation with clinical retinopathy of prematurity, Proc. Natl. Acad. Sci. U.S.A. 98 (2001) 5804–5808, https://doi.org/10.1073/pnas.101113998.
[11] T. Alon, I. Hemo, A. Itin, J. Pe'er, J. Stone, E. Keshet, Vascular endothelial growth factor acts as a survival factor for newly formed retinal vessels and has implications for retinopathy of prematurity, Nat. Med. 1 (1995) 1024–1028, https://doi.org/10.1038/nm1095-1024.
[12] T. Chan-Ling, B. Gock, J. Stone, The effect of oxygen on vasoformative cell division. Evidence that 'physiological hypoxia' is the stimulus for normal retinal vasculogenesis, Invest. Ophthalmol. Vis. Sci. 36 (1995) 1201–1214.
[13] J. Stone, A. Itin, T. Alon, J. Pe'er, H. Gnessin, T. Chan-Ling, E. Keshet, Development of retinal vasculature is mediated by hypoxia-induced vascular endothelial growth factor (VEGF) expression by neuroglia, J. Neurosci. 15 (1995) 4738–4747, https://doi.org/10.1523/jneurosci.15-07-04738.1995.
[14] E.A. Pierce, R.L. Avery, E.D. Foley, L.P. Aiello, L.E. Smith, Vascular endothelial growth factor/vascular permeability factor expression in a mouse model of retinal neovascularization, Proc. Natl. Acad. Sci. U.S.A. 92 (1995) 905–909, https://doi.org/10.1073/pnas.92.3.905.
[15] C. He, Y. Liu, Z. Huang, Z. Yang, T. Zhou, S. Liu, Z. Hao, J. Wang, Q. Feng, Y. Liu, et al., A specific RIP3(+) subpopulation of microglia promotes retinopathy through a hypoxia-triggered necroptotic mechanism, Proc. Natl. Acad. Sci. U.S.A. 118 (2021), https://doi.org/10.1073/pnas.2023290118.
[16] C.Q. Liu, X.Y. Liu, P.W. Ouyang, Q. Liu, X.M. Huang, F. Xiao, Y.H. Cui, Q. Zhou, H. W. Pan, Ferrostatin-1 attenuates pathological angiogenesis in oxygen-induced retinopathy via inhibition of ferroptosis, Exp. Eye Res. 226 (2023) 109347, https://doi.org/10.1016/j.exer.2022.109347.
[17] S. Sivaprasad, S. Sen, J. Cunha-Vaz, Perspectives of diabetic retinopathy-challenges and opportunities, Eye (Lond) 37 (2023) 2183–2191, https://doi.org/10.1038/s41433-022-02335-5.
[18] W. Zhang, J. Geng, A. Sang, Effectiveness of panretinal photocoagulation plus intravitreal anti-VEGF treatment against prp alone for diabetic retinopathy: a systematic review with meta-analysis, Front. Endocrinol. 13 (2022) 807687, https://doi.org/10.3389/fendo.2022.807687.
[19] J. Balla, H.S. Jacob, G. Balla, K. Nath, J.W. Eaton, G.M. Vercellotti, Endothelial-cell heme uptake from heme proteins: induction of sensitization and desensitization to oxidant damage, Proc. Natl. Acad. Sci. U.S.A. 90 (1993) 9285–9289, https://doi.org/10.1073/pnas.90.20.9285.
[20] D.A. Svistunenko, R.P. Patel, S.V. Voloshchenko, M.T. Wilson, The globin-based free radical of ferryl hemoglobin is detected in normal human blood, J. Biol. Chem. 272 (1997) 7114–7121, https://doi.org/10.1074/jbc.272.11.7114.
[21] R.P. Patel, D.A. Svistunenko, V.M. Darley-Usmar, M.C. Symons, M.T. Wilson, Redox cycling of human methaemoglobin by H2O2 yields persistent ferryl iron and protein based radicals, Free Radic. Res. 25 (1996) 117–123, https://doi.org/10.3109/10715769609149916.
[22] J.H. Crawford, B.K. Chacko, C.G. Kevil, R.P. Patel, The red blood cell and vascular function in health and disease, Antioxidants Redox Signal. 6 (2004) 992–999, https://doi.org/10.1089/ars.2004.6.992.
[23] W. Tarnow-Mordi, A. Kirby, Current recommendations and practice of oxygen therapy in preterm infants, Clin. Perinatol. 46 (2019) 621–636, https://doi.org/10.1016/j.clp.2019.05.015.
[24] D. Ley, B. Hallberg, I. Hansen-Pupp, C. Dani, L.A. Ramenghi, N. Marlow, K. Beardsall, F. Bhatti, D. Dunger, J.D. Higginson, et al., rhIGF-1/rhIGFBP-3 in preterm infants: a phase 2 randomized controlled trial, J. Pediatr. 206 (2019) 56–65.e58, https://doi.org/10.1016/j.jpeds.2018.10.033.
[25] L.P. Aiello, E.A. Pierce, E.D. Foley, H. Takagi, H. Chen, L. Riddle, N. Ferrara, G. L. King, L.E. Smith, Suppression of retinal neovascularization in vivo by inhibition of vascular endothelial growth factor (VEGF) using soluble VEGF-receptor chimeric proteins, Proc. Natl. Acad. Sci. U.S.A. 92 (1995) 10457–10461, https://doi.org/10.1073/pnas.92.23.10457.
[26] F.M. Mutlu, S.U. Sarici, Treatment of retinopathy of prematurity: a review of conventional and promising new therapeutic options, Int. J. Ophthalmol. 6 (2013) 228–236, https://doi.org/10.3980/j.issn.2222-3959.2013.02.23.
[27] T. Murakami, F. Okamoto, T. Kinoshita, K. Shinomiya, T. Nishi, S. Obata, S. Ogura, Y. Nishihara, H. Tsukitome, T. Jujo, et al., Comparison of long-term treatment outcomes of laser and anti-VEGF therapy in retinopathy of prematurity: a multicentre study from J-CREST group, Eye (Lond) (2023), https://doi.org/10.1038/s41433-023-02559-z.
[28] B.P. Nicholson, A.P. Schachat, A review of clinical trials of anti-VEGF agents for diabetic retinopathy, Graefes Arch. Clin. Exp. Ophthalmol. 248 (2010) 915–930, https://doi.org/10.1007/s00417-010-1315-z.
[29] G. Bindea, B. Mlecnik, H. Hackl, P. Charoentong, M. Tosolini, A. Kirilovsky, W. H. Fridman, F. Pagès, Z. Trajanoski, J. Galon, ClueGO: a Cytoscape plug-in to decipher functionally grouped gene ontology and pathway annotation networks, Bioinformatics 25 (2009) 1091–1093, https://doi.org/10.1093/bioinformatics/btp101.
[30] A.P. Levy, Hypoxic regulation of VEGF mRNA stability by RNA-binding proteins, Trends Cardiovasc. Med. 8 (1998) 246–250, https://doi.org/10.1016/s1050-1738(98)00020-6.
[31] H. Takagi, G.L. King, L.P. Aiello, Hypoxia upregulates glucose transport activity through an adenosine-mediated increase of GLUT1 expression in retinal capillary endothelial cells, Diabetes 47 (1998) 1480–1488, https://doi.org/10.2337/diabetes.47.9.1480.
[32] J.W. Kim, I. Tchernyshyov, G.L. Semenza, C.V. Dang, HIF-1-mediated expression of pyruvate dehydrogenase kinase: a metabolic switch required for cellular adaptation to hypoxia, Cell Metabol. 3 (2006) 177–185, https://doi.org/10.1016/j.cmet.2006.02.002.
[33] L. Lu, C.P. Seidel, T. Iwase, R.K. Stevens, Y.Y. Gong, X. Wang, S.F. Hackett, P. A. Campochiaro, Suppression of GLUT1; a new strategy to prevent diabetic complications, J. Cell. Physiol. 228 (2013) 251–257, https://doi.org/10.1002/jcp.24133.
[34] K. Sato, S. Mochida, D. Tomimoto, T. Konuma, N. Kiyota, S. Tsuda, Y. Shiga, K. Omodaka, T. Nakazawa, A pyruvate dehydrogenase kinase inhibitor prevents retinal cell death and improves energy metabolism in rat retinas after ischemia/reperfusion injury, Exp. Eye Res. 193 (2020) 107997, https://doi.org/10.1016/j.exer.2020.107997.
[35] A. Jozkowicz, I. Huk, A. Nigisch, G. Weigel, F. Weidinger, J. Dulak, Effect of prostaglandin-J(2) on VEGF synthesis depends on the induction of heme oxygenase-1, Antioxidants Redox Signal. 4 (2002) 577–585, https://doi.org/10.1089/15230860260220076.
[36] H.H. Lin, Y.H. Chen, P.F. Chang, Y.T. Lee, S.F. Yet, L.Y. Chau, Heme oxygenase-1 promotes neovascularization in ischemic heart by coinduction of VEGF and SDF-1, J. Mol. Cell. Cardiol. 45 (2008) 44–55, https://doi.org/10.1016/j.yjmcc.2008.04.011.
[37] C.C. Cheng, S.S. Guan, H.J. Yang, C.C. Chang, T.Y. Luo, J. Chang, A.S. Ho, Blocking heme oxygenase-1 by zinc protoporphyrin reduces tumor hypoxia-mediated VEGF release and inhibits tumor angiogenesis as a potential therapeutic agent against colorectal cancer, J. Biomed. Sci. 23 (2016) 18, https://doi.org/10.1186/s12929-016-0219-6.
[38] J. Dulak, A. Józkowicz, R. Foresti, A. Kasza, M. Frick, I. Huk, C.J. Green, O. Pachinger, F. Weidinger, R. Motterlini, Heme oxygenase activity modulates vascular endothelial growth factor synthesis in vascular smooth muscle cells, Antioxidants Redox Signal. 4 (2002) 229–240, https://doi.org/10.1089/152308602753666280.
[39] M.V. Kumar, C.N. Nagineni, M.S. Chin, J.J. Hooks, B. Detrick, Innate immunity in the retina: toll-like receptor (TLR) signaling in human retinal pigment epithelial cells, J. Neuroimmunol. 153 (2004) 7–15, https://doi.org/10.1016/j.jneuroim.2004.04.018.
[40] N. Bayan, N. Yazdanpanah, N. Rezaei, Role of toll-like receptor 4 in diabetic retinopathy, Pharmacol. Res. 175 (2022) 105960, https://doi.org/10.1016/j.phrs.2021.105960.
[41] H. Fu, H. Liu, Deletion of toll-like receptor 4 ameliorates diabetic retinopathy in mice, Arch. Physiol. Biochem. 129 (2023) 519–525, https://doi.org/10.1080/13813455.2020.1841795.
[42] R.T. Figueiredo, P.L. Fernandez, D.S. Mourao-Sa, B.N. Porto, F.F. Dutra, L.S. Alves, M.F. Oliveira, P.L. Oliveira, A.V. Graça-Souza, M.T. Bozza, Characterization of heme as activator of Toll-like receptor 4, J. Biol. Chem. 282 (2007) 20221–20229, https://doi.org/10.1074/jbc.M610737200.
[43] R. Fukuda, K. Hirota, F. Fan, Y.D. Jung, L.M. Ellis, G.L. Semenza, Insulin-like growth factor 1 induces hypoxia-inducible factor 1-mediated vascular endothelial growth factor expression, which is dependent on MAP kinase and phosphatidylinositol 3-kinase signaling in colon cancer cells, J. Biol. Chem. 277 (2002) 38205–38211, https://doi.org/10.1074/jbc.M203781200.
[44] B.H. Jiang, G. Jiang, J.Z. Zheng, Z. Lu, T. Hunter, P.K. Vogt, Phosphatidylinositol 3-kinase signaling controls levels of hypoxia-inducible factor 1, Cell Growth Differ. 12 (2001) 363–369.
[45] E. Laughner, P. Taghavi, K. Chiles, P.C. Mahon, G.L. Semenza, HER2 (neu) signaling increases the rate of hypoxia-inducible factor 1alpha (HIF-1alpha) synthesis: novel mechanism for HIF-1-mediated vascular endothelial growth factor expression, Mol. Cell Biol. 21 (2001) 3995–4004, https://doi.org/10.1128/mcb.21.12.3995-4004.2001.
[46] J. Karar, A. Maity, PI3K/AKT/mTOR pathway in angiogenesis, Front. Mol. Neurosci. 4 (2011) 51, https://doi.org/10.3389/fnmol.2011.00051.
[47] D.R. Alessi, M. Andjelkovic, B. Caudwell, P. Cron, N. Morrice, P. Cohen, B. A. Hemmings, Mechanism of activation of protein kinase B by insulin and IGF-1, EMBO J. 15 (1996) 6541–6551, https://doi.org/10.1002/j.1460-2075.1996.tb01045.x.
[48] S. Semba, N. Itoh, M. Ito, M. Harada, M. Yamakawa, The in vitro and in vivo effects of 2-(4-morpholinyl)-8-phenyl-chromone (LY294002), a specific inhibitor of phosphatidylinositol 3'-kinase, in human colon cancer cells, Clin. Cancer Res. 8 (2002) 1957–1963.
[49] A. Stahl, L. Paschek, G. Martin, N.J. Gross, N. Feltgen, L.L. Hansen, H.T. Agostini, Rapamycin reduces VEGF expression in retinal pigment epithelium (RPE) and

inhibits RPE-induced sprouting angiogenesis in vitro, FEBS Lett. 582 (2008) 3097–3102, https://doi.org/10.1016/j.febslet.2008.08.005.
[50] X. Jiang, Y. Wei, T. Zhang, Z. Zhang, S. Qiu, X. Zhou, S. Zhang, Effects of GSK2606414 on cell proliferation and endoplasmic reticulum stress-associated gene expression in retinal pigment epithelial cells, Mol. Med. Rep. 15 (2017) 3105–3110, https://doi.org/10.3892/mmr.2017.6418.
[51] Q. Zhong, R.A. Kowluru, Diabetic retinopathy and damage to mitochondrial structure and transport machinery, Invest. Ophthalmol. Vis. Sci. 52 (2011) 8739–8746, https://doi.org/10.1167/iovs.11-8045.
[52] R.A. Kowluru, M. Mishra, Oxidative stress, mitochondrial damage and diabetic retinopathy, Biochim. Biophys. Acta 1852 (2015) 2474–2483, https://doi.org/10.1016/j.bbadis.2015.08.001.
[53] F.A. Siddiqui, H. Desai, T.F. Siddiqui, J.L. Francis, Hemoglobin induces the expression and secretion of vascular endothelial growth factor from human malignant cells, Hematol J 3 (2002) 264–270, https://doi.org/10.1038/sj.thj.6200190.
[54] K.A. Hutcheson, A.T. Nguyen, M.W. Preslan, N.J. Ellish, S.M. Steidl, Vitreous hemorrhage in patients with high-risk retinopathy of prematurity, Am. J. Ophthalmol. 136 (2003) 258–263, https://doi.org/10.1016/s0002-9394(03)00190-9.
[55] R.S. Araújo, D.F. Santos, G.A. Silva, The role of the retinal pigment epithelium and Müller cells secretome in neovascular retinal pathologies, Biochimie 155 (2018) 104–108, https://doi.org/10.1016/j.biochi.2018.06.019.
[56] Y. Sun, C.H. Liu, J.P. SanGiovanni, L.P. Evans, K.T. Tian, B. Zhang, A. Stahl, W. T. Pu, T.M. Kamenecka, L.A. Solt, et al., Nuclear receptor RORα regulates pathologic retinal angiogenesis by modulating SOCS3-dependent inflammation, Proc. Natl. Acad. Sci. U.S.A. 112 (2015) 10401–10406, https://doi.org/10.1073/pnas.1504387112.
[57] X. Yang, J. Cao, Y. Du, Q. Gong, Y. Cheng, G. Su, Angiopoietin-like protein 4 (ANGPTL4) induces retinal pigment epithelial barrier breakdown by activating signal transducer and activator of transcription 3 (STAT3): evidence from ARPE-19 cells under hypoxic condition and diabetic rats, Med. Sci. Mon. Int. Med. J. Exp. Clin. Res. 25 (2019) 6742–6754, https://doi.org/10.12659/msm.915748.
[58] C.M. Sorenson, S. Wang, R. Gendron, H. Paradis, N. Sheibani, Thrombospondin-1 deficiency exacerbates the pathogenesis of diabetic retinopathy, J. Diabetes Metabol. 12 (2013), https://doi.org/10.4172/2155-6156.S12-005.
[59] C.L. Zhang, H.L. Wang, P.C. Li, C.D. Hong, A.Q. Chen, Y.M. Qiu, A.P. Zeng, Y. F. Zhou, B. Hu, Y.N. Li, Mfsd2a overexpression alleviates vascular dysfunction in diabetic retinopathy, Pharmacol. Res. 171 (2021) 105755, https://doi.org/10.1016/j.phrs.2021.105755.
[60] M.G. Petrovic, P. Korosec, M. Kosnik, M. Hawlina, Vitreous levels of interleukin-8 in patients with proliferative diabetic retinopathy, Am. J. Ophthalmol. 143 (2007) 175–176, https://doi.org/10.1016/j.ajo.2006.07.032.
[61] D. Li, J. Tang, R. Gao, J. Lan, W. Shen, Y. Liu, Y. Chen, H. Sun, J. Yan, Y. Nie, et al., PFKFB4 promotes angiogenesis via IL-6/STAT5A/P-STAT5 signaling in breast cancer, J. Cancer 13 (2022) 212–224, https://doi.org/10.7150/jca.66773.
[62] Y. Wang, C. Yang, Q. Gu, M. Sims, W. Gu, L.M. Pfeffer, J. Yue, KLF4 promotes angiogenesis by activating VEGF signaling in human retinal microvascular endothelial cells, PLoS One 10 (2015) e0130341, https://doi.org/10.1371/journal.pone.0130341.
[63] R.K. Vadlapatla, A.D. Vadlapudi, A.K. Mitra, Hypoxia-inducible factor-1 (HIF-1): a potential target for intervention in ocular neovascular diseases, Curr. Drug Targets 14 (2013) 919–935, https://doi.org/10.2174/13894501113149990015.
[64] D. Zhang, F.L. Lv, G.H. Wang, Effects of HIF-1α on diabetic retinopathy angiogenesis and VEGF expression, Eur. Rev. Med. Pharmacol. Sci. 22 (2018) 5071–5076, https://doi.org/10.26355/eurrev_201808_15699.
[65] Y. Jiang, J. Wu, R.F. Keep, Y. Hua, J.T. Hoff, G. Xi, Hypoxia-inducible factor-1alpha accumulation in the brain after experimental intracerebral hemorrhage, J. Cerebr. Blood Flow Metabol. 22 (2002) 689–696, https://doi.org/10.1097/00004647-200206000-00007.
[66] M. Shahidatul-Adha, E. Zunaina, M.N. Aini-Amalina, Evaluation of vascular endothelial growth factor (VEGF) level in the tears and serum of age-related macular degeneration patients, Sci. Rep. 12 (2022) 4423, https://doi.org/10.1038/s41598-022-08492-7.
[67] S. Rutardottir, E. Karnaukhova, C. Nantasenamat, N. Songtawee, V. Prachayasittikul, M. Rajabi, L.W. Rosenlöf, A.I. Alayash, B. Åkerström, Structural and biochemical characterization of two heme binding sites on α1-microglobulin using site directed mutagenesis and molecular simulation, Biochim. Biophys. Acta 1864 (2016) 29–41, https://doi.org/10.1016/j.bbapap.2015.10.002.
[68] G. Cavallaro, L. Filippi, P. Bagnoli, G. La Marca, G. Cristofori, G. Raffaeli, L. Padrini, G. Araimo, M. Fumagalli, M. Groppo, et al., The pathophysiology of retinopathy of prematurity: an update of previous and recent knowledge, Acta Ophthalmol. 92 (2014) 2–20, https://doi.org/10.1111/aos.12049.
[69] X. Wang, G. Wang, Y. Wang, Intravitreous vascular endothelial growth factor and hypoxia-inducible factor 1a in patients with proliferative diabetic retinopathy, Am. J. Ophthalmol. 148 (2009) 883–889, https://doi.org/10.1016/j.ajo.2009.07.007.
[70] E. Chang, A.S. Josan, R. Purohit, C.K. Patel, K. Xue, A network meta-analysis of retreatment rates following bevacizumab, ranibizumab, aflibercept, and laser for retinopathy of prematurity, Ophthalmology 129 (2022) 1389–1401, https://doi.org/10.1016/j.ophtha.2022.06.042.
[71] G. Uludag, M. Hassan, W. Matsumiya, B.H. Pham, S. Chea, N. Trong Tuong Than, H.L. Doan, A. Akhavanrezayat, M.S. Halim, D.V. Do, et al., Efficacy and safety of intravitreal anti-VEGF therapy in diabetic retinopathy: what we have learned and what should we learn further? Expet Opin. Biol. Ther. 22 (2022) 1275–1291, https://doi.org/10.1080/14712598.2022.2100694.
[72] J.A. Zehden, X.M. Mortensen, A. Reddy, A.Y. Zhang, Systemic and ocular adverse events with intravitreal anti-VEGF therapy used in the treatment of diabetic retinopathy: a review, Curr. Diabetes Rep. 22 (2022) 525–536, https://doi.org/10.1007/s11892-022-01491-y.
[73] Y. Alvarez, O. Astudillo, L. Jensen, A.L. Reynolds, N. Waghorne, D.P. Brazil, Y. Cao, J.J. O'Connor, B.N. Kennedy, Selective inhibition of retinal angiogenesis by targeting PI3 kinase, PLoS One 4 (2009) e7867, https://doi.org/10.1371/journal.pone.0007867.
[74] Y. Di, X.L. Chen, Inhibition of LY294002 in retinal neovascularization via down-regulation the PI3K/AKT-VEGF pathway in vivo and in vitro, Int. J. Ophthalmol. 11 (2018) 1284–1289, https://doi.org/10.18240/ijo.2018.08.06.
[75] G.J. Brunn, J. Williams, C. Sabers, G. Wiederrecht, J.C. Lawrence Jr., R. T. Abraham, Direct inhibition of the signaling functions of the mammalian target of rapamycin by the phosphoinositide 3-kinase inhibitors, wortmannin and LY294002, EMBO J. 15 (1996) 5256–5267, https://doi.org/10.1002/j.1460-2075.1996.tb00911.x.
[76] Y.Z. Sun, L. Liu, N. Cai, N.N. Liu, Anti-angiogenic effect of rapamycin in mouse oxygen-induced retinopathy is mediated through suppression of HIF-1alpha/VEGF pathway, Int. J. Clin. Exp. Pathol. 10 (2017) 10167–10175.
[77] J. Wei, H. Jiang, H. Gao, G. Wang, Blocking mammalian target of rapamycin (mTOR) attenuates HIF-1α pathways engaged-vascular endothelial growth factor (VEGF) in diabetic retinopathy, Cell. Physiol. Biochem. 40 (2016) 1570–1577, https://doi.org/10.1159/000453207.
[78] D.Q. Kong, L. Li, Y. Liu, G.Y. Zheng, Association between endoplasmic reticulum stress and risk factors of diabetic retinopathy, Int. J. Ophthalmol. 11 (2018) 1704–1710, https://doi.org/10.18240/ijo.2018.10.20.
[79] Y. Hu, X. Lu, Y. Xu, L. Lu, S. Yu, Q. Cheng, B. Yang, C.K. Tsui, D. Ye, J. Huang, et al., Salubrinal attenuated retinal neovascularization by inhibiting CHOP-HIF1α-VEGF pathways, Oncotarget 8 (2017) 77219–77232, https://doi.org/10.18632/oncotarget.20431.
[80] D. Pethő, Z. Hendrik, A. Nagy, L. Beke, A. Patsalos, L. Nagy, S. Póliska, G. Méhes, C. Tóth, L. Potor, et al., Heme cytotoxicity is the consequence of endoplasmic reticulum stress in atherosclerotic plaque progression, Sci. Rep. 11 (2021) 10435, https://doi.org/10.1038/s41598-021-89713-3.
[81] J. Blasiak, G. Petrovski, Z. Veréb, A. Facskó, K. Kaarniranta, Oxidative stress, hypoxia, and autophagy in the neovascular processes of age-related macular degeneration, BioMed Res. Int. 2014 (2014) 768026, https://doi.org/10.1155/2014/768026.
[82] G.B. Arden, S. Sivaprasad, Hypoxia and oxidative stress in the causation of diabetic retinopathy, Curr. Diabetes Rev. 7 (2011) 291–304, https://doi.org/10.2174/157339911797415620.
[83] G. Balla, H.S. Jacob, J. Balla, M. Rosenberg, K. Nath, F. Apple, J.W. Eaton, G. M. Vercellotti, Ferritin: a cytoprotective antioxidant strategem of endothelium, J. Biol. Chem. 267 (1992) 18148–18153, https://doi.org/10.1016/S0021-9258(19)37165-0.
[84] P. Ellinghaus, I. Heisler, K. Unterschemmann, M. Haerter, H. Beck, S. Greschat, A. Ehrmann, H. Summer, I. Flamme, F. Oehme, et al., BAY 87-2243, a highly potent and selective inhibitor of hypoxia-induced gene activation has antitumor activities by inhibition of mitochondrial complex I, Cancer Med. 2 (2013) 611–624, https://doi.org/10.1002/cam4.112.
[85] T. Kurihara, P.D. Westenskow, M.L. Gantner, Y. Usui, A. Schultz, S. Bravo, E. Aguilar, C. Wittgrove, M. Friedlander, L.P. Paris, et al., Hypoxia-induced metabolic stress in retinal pigment epithelial cells is sufficient to induce photoreceptor degeneration, Elife 5 (2016), https://doi.org/10.7554/eLife.14319.
[86] D. Park, P.J. Dilda, Mitochondria as targets in angiogenesis inhibition, Mol. Aspect. Med. 31 (2010) 113–131, https://doi.org/10.1016/j.mam.2009.12.005.
[87] D. Guo, Q. Wang, C. Li, Y. Wang, X. Chen, VEGF stimulated the angiogenesis by promoting the mitochondrial functions, Oncotarget 8 (2017) 77020–77027, https://doi.org/10.18632/oncotarget.20331.
[88] Y. Wang, Q.S. Zang, Z. Liu, Q. Wu, D. Maass, G. Dulan, P.W. Shaul, L. Melito, D. E. Frantz, J.A. Kilgore, et al., Regulation of VEGF-induced endothelial cell migration by mitochondrial reactive oxygen species, Am. J. Physiol. Cell Physiol. 301 (2011) C695–C704, https://doi.org/10.1152/ajpcell.00322.2010.
[89] T. Gáll, G. Balla, J. Heme Balla, Heme oxygenase, and endoplasmic reticulum stress-A new insight into the pathophysiology of vascular diseases, Int. J. Mol. Sci. 20 (2019), https://doi.org/10.3390/ijms20153675.
[90] A.P. Adamis, D.T. Shima, K.T. Yeo, T.K. Yeo, L.F. Brown, B. Berse, P.A. D'Amore, J. Folkman, Synthesis and secretion of vascular permeability factor/vascular endothelial growth factor by human retinal pigment epithelial cells, Biochem. Biophys. Res. Commun. 193 (1993) 631–638, https://doi.org/10.1006/bbrc.1993.1671.
[91] C. Schwesinger, C. Yee, R.M. Rohan, A.M. Joussen, A. Fernandez, T.N. Meyer, V. Poulaki, J.J. Ma, T.M. Redmond, S. Liu, et al., Intrachoroidal neovascularization in transgenic mice overexpressing vascular endothelial growth factor in the retinal pigment epithelium, Am. J. Pathol. 158 (2001) 1161–1172, https://doi.org/10.1016/s0002-9440(10)64063-1.
[92] K. Spilsbury, K.L. Garrett, W.Y. Shen, I.J. Constable, P.E. Rakoczy, Overexpression of vascular endothelial growth factor (VEGF) in the retinal pigment epithelium leads to the development of choroidal neovascularization, Am. J. Pathol. 157 (2000) 135–144, https://doi.org/10.1016/s0002-9440(10)64525-7.
[93] J.C. Rivera, M. Holm, D. Austeng, T.S. Morken, T.E. Zhou, A. Beaudry-Richard, E. M. Sierra, O. Dammann, S. Chemtob, Retinopathy of prematurity: inflammation, choroidal degeneration, and novel promising therapeutic strategies, J. Neuroinflammation 14 (2017) 165, https://doi.org/10.1186/s12974-017-0943-1.

[94] The international classification of retinopathy of prematurity revisited, Arch. Ophthalmol. 123 (2005) 991–999, https://doi.org/10.1001/archopht.123.7.991.
[95] M.F. Chiang, G.E. Quinn, A.R. Fielder, S.R. Ostmo, R.V. Paul Chan, A. Berrocal, G. Binenbaum, M. Blair, J. Peter Campbell, A. Capone Jr., et al., International classification of retinopathy of prematurity, third edition, Ophthalmology 128 (2021) e51–e68, https://doi.org/10.1016/j.ophtha.2021.05.031.
[96] W.V. Good, R.J. Hardy, V. Dobson, E.A. Palmer, D.L. Phelps, B. Tung, M. Redford, Final visual acuity results in the early treatment for retinopathy of prematurity study, Arch. Ophthalmol. 128 (2010) 663–671, https://doi.org/10.1001/archophthalmol.2010.72.
[97] G. Silva, V. Jeney, A. Chora, R. Larsen, J. Balla, M.P. Soares, Oxidized hemoglobin is an endogenous proinflammatory agonist that targets vascular endothelial cells, J. Biol. Chem. 284 (2009) 29582–29595, https://doi.org/10.1074/jbc.M109.045344.
[98] C.C. Winterbourn, Oxidative reactions of hemoglobin, Methods Enzymol. 186 (1990) 265–272, https://doi.org/10.1016/0076-6879(90)86118-f.
[99] E. Nagy, J.W. Eaton, V. Jeney, M.P. Soares, Z. Varga, Z. Galajda, J. Szentmiklósi, G. Méhes, T. Csonka, A. Smith, et al., Red cells, hemoglobin, heme, iron, and atherogenesis, Arterioscler. Thromb. Vasc. Biol. 30 (2010) 1347–1353, https://doi.org/10.1161/atvbaha.110.206433.